4

On the Role of the Gulf Stream in the Changing Atlantic Nutrient Circulation During the 21st Century

Daniel B. Whitt

ABSTRACT

The Gulf Stream transports macronutrients poleward as a part of the Atlantic meridional overturning circulation (AMOC). Scaling shows that this advective transport is greater than diapycnal transport from deep convection in the North Atlantic and is therefore crucial for sustaining the nutrient supply to the subpolar North Atlantic on interannual timescales. Simulations of the RCP8.5 emissions scenario with the Community Earth System Model (CESM) reveal 25% declines in the Gulf Stream volume transport above the potential density surface $\sigma_\theta = 27.5\,\mathrm{kg/m^3}$ and 35% declines in the associated nitrate transport between 2006 and 2080. The declining Gulf Stream transport largely explains contemporaneous 40% declines in zonally-integrated volume and nitrate transports in the subtropical part of the AMOC. In addition, scaling suggests that the declining Gulf Stream nitrate transport (2.4 kmol/s per year) is the dominant driver of the declining export of particulate organic nitrogen across $\sigma_\theta = 27.5\,\mathrm{kg/m^3}$ in the subpolar North Atlantic (0.57 kmol/s per year), because the declining nitrate entrainment from water with $\sigma_\theta > 27.5\,\mathrm{kg/m^3}$ is only 0.44 kmol/s per year. A review of various small-scale ocean physical processes suggests that the projected decline in the Gulf Stream nutrient flux is qualitatively robust to uncertainties associated with ocean physics.

4.1. INTRODUCTION

The Gulf Stream is part of the upper limb of the Atlantic meridional overturning circulation (AMOC) and the western boundary current of the North Atlantic subtropical gyre. The Gulf Stream is also a nutrient stream. It transports macronutrients (nitrate, phosphate, silicate) necessary for marine phytoplankton growth along the eastern continental margin of the United States from the Straits of Florida to Cape Hatteras at globally significant rates. At Cape Hatteras, the Gulf Stream separates from the coast and carries its nutrients to the northeast off the continental slope and into deep water. There, waters of recent tropical, subtropical and subpolar origins converge and both the volume and nutrient transport increase in a great junction of the global ocean circulation. Further east, near the Grand Banks of Newfoundland, the waters and nutrients of the Gulf Stream diverge again into the subtropical and subpolar gyres.

As nutrients and water move northward, they rise along sloping isopycnals and are eventually advected into the surface mixed layer or entrained by seasonal mixed-layer deepening. This upwards nutrient flux is compensated for by downwards nutrient fluxes associated with physical and biogeochemical processes. A significant fraction of the inorganic nutrient entering the mixed layer is transformed directly to denser North Atlantic Deep Water and sinks as the incoming water loses heat to the atmosphere. However, another significant fraction of the inorganic nutrient entering the mixed layer is converted to organic form by phytoplankton. A fraction of this organic nutrient sinks via particles to denser water, where it is remineralized, and the other fraction of the organic nutrient (i.e., the nonsinking dissolved part) is transformed

National Center for Atmospheric Research, Boulder, CO, USA

Kuroshio Current: Physical, Biogeochemical, and Ecosystem Dynamics, Geophysical Monograph 243, First Edition.
Edited by Takeyoshi Nagai, Hiroaki Saito, Koji Suzuki, and Motomitsu Takahashi.

to denser water by physical processes and then remineralized. This basin-scale circulation of nutrients strongly influences biogeochemistry in the subpolar North Atlantic. The high rate of upwelling is necessary to support high levels of new primary production, and this upwelling indirectly or directly influences phytoplankton phenology, higher trophic levels of marine ecosystems, and air–sea carbon dioxide fluxes.

A brief scaling exercise, based on results summarized in Table 4.1, demonstrates the significance of the Gulf Stream for the global nutrient circulation. The maximum advective nitrate flux associated with the Gulf Stream is about 700 − 800 kmol/s above the potential density surface $\sigma_\theta = 27.5\,\mathrm{kg/m^3}$, and the minimum flux, through the Straits of Florida, is about 300 kmol/s (Pelegrí & Csanady, 1991; Pelegrí et al., 1996, 2006; Williams et al., 2011). This isopycnal $\sigma_\theta = 27.5\,\mathrm{kg/m^3}$ is at about 1 km depth in the subtropics and outcrops in the subpolar gyre near sites of deep convection. In addition, the northward AMOC transport occurs approximately where $\sigma_\theta < 27.5\,\mathrm{kg/m^3}$ and the southward AMOC transport occurs approximately where $\sigma_\theta > 27.5\,\mathrm{kg/m^3}$ (Lumpkin & Speer, 2007). To put this maximum advective nitrate flux in perspective, it is about 40 times larger than the interior diapycnal nitrate flux across the main pycnocline integrated over the entire North Atlantic, ∼20 kmol/s, assuming a canonical open-ocean turbulent diapycnal diffusivity of 10^{-5} m²/s (Ledwell et al., 1993; Waterhouse et al., 2014), a typical vertical nitrate gradient of 5×10^{-5} mol/m⁴, and an area of 40 million km². The diabatic volume transformation associated with this mixing (only a couple of Sv) is quantitatively consistent with current best estimates of the internal wave driven diabatic volume transformation (Kunze, 2017). This consistency supports the hypothesis that the majority of the volume transport passing through the Gulf Stream that is associated with AMOC (about 15 Sv (Lumpkin & Speer, 2007), only a small fraction of the total Gulf Stream volume transport) is not associated with diabatic watermass transformations driven by internal wave breaking in the pycnocline. Rather, the AMOC mostly flows along isopycnals in the pycnocline and watermass transformations occur in surface boundary layers of the subpolar North and South Atlantic (Toggweiler & Samuels, 1998; Marshall & Speer, 2012). On the other hand, the maximum Gulf Stream advective nitrate flux above $\sigma_\theta = 27.5\,\mathrm{kg/m^3}$ is only twice as large as the zonally-integrated flux above $\sigma_\theta = 27.5\,\mathrm{kg/m^3}$ at 36° N, which is about 350 kmol/s, because the northward Gulf Stream transport is correlated with higher nitrate concentrations and the southward shallow return flow in the gyre interior is correlated with lower nitrate concentrations (Rintoul & Wunsch, 1991). In addition, the maximum Gulf Stream advective flux is about 10 times larger than the time-averaged nitrate flux upwards across $\sigma_\theta = 27.5\,\mathrm{kg/m^3}$ due to wintertime convection and subsequent restratification, ∼50–75 kmol/s. This convective flux is obtained by assuming an annual increase in upper-ocean nitrate of 1.0–1.4 mol/m²-yr (Williams et al., 2000), of which about half is sourced from water denser than $\sigma_\theta = 27.5\,\mathrm{kg/m^3}$ (this fraction from $\sigma_\theta > 27.5\,\mathrm{kg/m^3}$ is based on the Earth system model results reported below; see Table 4.2). To put this 1.0–1.4 mol/m²-yr flux in perspective, it would resupply 10–14 mmol/m³ of nitrate over the top 100 m of the water column each year.

Table 4.1 Summary of Data and Model Results Relevant to Scaling the Nitrate Budget of the Subpolar North Atlantic.

Quantity	Range of possible values	References
Separated GS adv. flux near 36° N, $\sigma_\theta < 27.5\,\mathrm{kg/m^3}$	(692.4, 788.6) kmol/s	2 sections, (Pelegrí & Csanady, 1991; Williams et al., 2011)
Florida Straits adv. flux, $\sigma_\theta < 27.5\,\mathrm{kg/m^3}$	(302.5, 303.0) kmol/s	2 sections, (Pelegrí & Csanady, 1991; Williams et al., 2011)
AMOC adv. flux at 36° N, $\sigma_\theta < 27.5\,\mathrm{kg/m^3}$	350 kmol/s	1 section, (Rintoul & Wunsch, 1991)
κ_ρ, below surface mixed layer, North Atlantic	$(3.7, 1.1, 1–5) \times 10^{-5}$ m²/s	(Lewis et al., 1986; Ledwell et al., 1993; Martin et al., 2010)
$\partial NO3/\partial z$, below surface mixed layer, North Atlantic	(0.045, 0.02–0.1, 0.03–0.1) mmol/m⁴	(Lewis et al., 1986; Martin et al., 2010); Fig. 3 (b) here
A_{NA} area of Atlantic 0–75° N, −70° to 10° E	39.9×10^6 km²	(Wessel & Smith, 1996)
A_{NA} area of Atlantic 45– 75° N, −70° to 10° E	11.0×10^6 km²	(Wessel & Smith, 1996)
Diffusive flux $\kappa \partial NO3/\partial z\, A_{NA}$	(8.0–200) kmol/s, (2.2–55) kmol/s	whole N. Atl. and subpolar N. Atl.
Area A_{en}, March $\sigma_\theta > 27.5$, 48–65° N	3.4×10^6 km²	WOA13 (Boyer et al., 2013)
Annual avg. entrainment flux F_{en}, March $\sigma_\theta > 27.5$	(1.0–1.4) mol/m²yr	(Williams et al., 2000), model means from 1968–1993
Area integrated entrainment, 48–65° N	(108–151) kmol/s	combining WOA13 A_{en} and Williams F_{en}

Table 4.2 Interquartile Ranges from the CESM1 Ensemble in 2006 and 2080*.

	AMOCN	AMOCV	PON275	PON100	EN	EN275	GS,64°W,N	GS,30.5°N,N	GS,64°W,V	GS,30.5°N,V	AREA	VOL	NO3
Year	kmol/s	Sv	kmol/s	kmol/s	kmol/s	kmol/s	kmol/s	kmol/s	Sv	Sv	$10^6 km^2$	$10^{15} m^3$	10^{10} kmol
2006	(303, 313)	(18.3, 19.3)	(76.8, 81.9)	(118, 123)	(66.1, 82.5)	(27.7, 42.7)	(521, 547)	(507, 528)	(35.9, 37.6)	(36.8, 38.8)	(4.3, 4.8)	(1.46,1.59)	(2.4, 2.6)
2080	(169,184)	(10.9, 12.0)	(32.6, 40.2)	(85, 90)	(5.2, 25.3)	(0.8, 2.4)	(337, 366)	(330, 347)	(26.6, 28.5)	(28.7, 30.0)	(0.5, 1.5)	(2.65, 2.94)	(3.9, 4.3)
percentage change	−43	−39	−54	−27	−79	−95	−34	−35	−25	−22	−78	+83	+64
rate of change/yr	−1.8	−0.10	−0.57	−0.44	−0.79	−0.44	−2.4	−2.4	−0.13	−0.11	−0.047	+.017	+.021

* Including: the zonally-integrated advective nitrate flux (AMOCN) and volume flux (AMOCV) across 48° N for $\sigma_\theta < 27.5\,kg/m^3$; the area-integrated export flux of particulate organic nitrogen north of 48°N and across $\sigma_\theta = 27.5\,kg/m^3$ or across 100 m depth, which is converted from carbon to nitrogen units by multiplying by 16/117 (PON275, PON100); the area-integrated entrainment flux north of 48°N, where March surface density $\sigma_\theta > 27.5\,kg/m^3$ (EN); the area-integrated entrainment flux north of 48°N sourced from water with density $\sigma_\theta > 27.5\,kg/m^3$ (EN275); advective nitrate (N) and volume (V) fluxes in two Gulf Stream sections summed above $\sigma_\theta < 27.5\,kg/m^3$, from 35–45° N at 64°W and out to 69°W at 30.5° N (see Figure 4.9). Other variables include: the area north of 48°N, where the surface density $\sigma_\theta > 27.5\,kg/m^3$ in March (AREA); the volume north of 48°N, where $\sigma_\theta < 27.5\,kg/m^3$ (VOL); and the nitrate reservoir north of 48°N and above $\sigma_\theta = 27.5\,kg/m^3$ (NO3).

Further, it is assumed that this convective flux occurs over an area of 3.4 million km^2, where $\sigma_\theta > 27.5\,\mathrm{kg/m^3}$ in March (Boyer et al., 2013). This area is about 40% larger than the combined area of the Norwegian and Labrador Seas, two main sites of deep convection in the subpolar North Atlantic (Marshall & Schott, 1999). Finally, the Gulf Stream advective nitrate flux is between one and two orders of magnitude larger than the estimated nitrate flux into the surface mixed layer due to the integrated effect of Ekman suction in the subpolar gyre (as quantified by Williams et al., 2006). In addition, it may be noted that eddies tend to oppose the Eulerian mean Ekman upwelling in the subpolar gyre, leading to an even smaller residual upwelling associated with the gyre circulation (McGillicuddy et al., 2003; Doddridge et al., 2016) than the Eulerian mean estimates of Williams et al. (2006).

Therefore, it has reasonably been hypothesized that the nearly-isopycnal advection of nutrients along the Gulf Stream is the dominant source of nutrients to the upper ocean ($\sigma_\theta < 27.5\,\mathrm{kg/m^3}$) in the mid-to-high latitude North Atlantic and should, therefore, approximately balance combined losses due to both biological processes (including sinking organic particles) or transformation (via diabatic processes in the ocean mixed layer) to water denser than $\sigma_\theta = 27.5\,\mathrm{kg/m^3}$ on interannual and longer timescales. Based on mean March isopycnal outcrop positions, it has been hypothesized that Gulf Stream nutrients on the relatively lighter isopycnal layers $\sigma_\theta < 26.8\,\mathrm{kg/m^3}$ irrigate the subtropics and intergyre boundary, whereas deeper isopycnals $26.8 < \sigma_\theta < 27.5$ irrigate the subpolar gyre (Pelegrí et al., 1996, 2006; Williams & Follows, 2003; Williams et al., 2006, 2011).

Thus, an important challenge, which has been recognized and worked on for many years (Rossby, 1936; Bower et al., 1985; Schmitz & McCartney, 1993; Brambilla & Talley, 2006; Williams et al., 2006; Pelegrí et al., 2006; Hakkinen & Rhines, 2009; Burkholder & Lozier, 2014; Lozier et al., 2017), is to observe and model the processes by which waters from different origins are transported by the Gulf Stream, modified by small-scale ($\lesssim$100 km) physical processes within the Gulf Stream, and then separated from the Gulf Stream onto different paths in the ocean circulation. In this chapter, some of what is currently known about the Gulf Stream nutrient stream is reviewed. Novel aspects include results from a large ensemble of 34 simulations from a single global Earth system model in the RCP8.5 21st century emissions scenario (Van Vuuren et al., 2011; Riahi et al., 2011) and an assessment of the role of various small scale ocean physical processes in sustaining the Gulf Stream nutrient transport, including the components associated with recirculating gyre transport and AMOC. In this context, small-scale processes are those that are unresolved (or poorly resolved) by global Earth system models and global-scale observing systems, such as interior diapycnal mixing, boundary layer mixing, and mesoscale processes. However, for context, the chapter begins with an observational description of the Gulf Stream nutrient stream.

4.2. A LARGE-SCALE OBSERVATIONAL DESCRIPTION OF THE GULF STREAM NUTRIENT STREAM

This section provides an observational description of the Gulf Stream nutrient stream, including Gulf Stream hydrography and velocity, nutrient concentration distribution, and nutrient transport. The sources, sinks, and ultimate fate of the Gulf Stream nutrients are also discussed.

4.2.1. Gulf Stream Hydrography and Velocity

The Gulf Stream is associated with a prominent surface front that has been recognized for several centuries and studied persistently for much of the last century (Rossby, 1936; Stommel, 1958; Palter et al., 2013). Like other large scale fronts, the Gulf Stream front can be identified by large horizontal gradients in many ocean tracers at a given depth and, equivalently, by large horizontal gradients in the depth of an isopleth of tracer concentration. For example, isopycnals shoal by hundreds of meters across the core of the Gulf Stream. Deeper isopycnals/isopleths are to the south and east of the stream, whereas shallower isopycnals/isopleths are to the north and west. Hence, maps of the depth of an isopycnal, like $\sigma_\theta = 26.95\,\mathrm{kg/m^3}$ shown in Figure 4.1, reveal the Gulf Stream path as tightly spaced contours from the Straits of Florida (27° N, 80° W) to southeast of the Grand Banks (40° N, 50° W).

These steeply sloping isopycnals are associated with a surface-intensified stream about 150 km wide and flowing to the northeast (about 90° to the right of the horizontal density gradient), as shown in Figures 4.2a and 4.2e. The stream is approximately in thermal wind balance, that is the baroclinic torque associated with steeply sloping isopycnals of the Gulf Stream front is balanced by the tilting of planetary vorticity by the vertically sheared horizontal flow (Stommel, 1958). But direct observations of the velocity and hydrography reveal a non-negligible $\sim$10% difference from thermal wind due to the centripetal acceleration associated with stream curvature and fast near-surface currents (Halkin & Rossby, 1985; Johns et al., 1989, 1995; Hogg, 1992). In addition, velocity observations reveal 5–10 cm/s streamwise velocities at 2 km depth, which are associated with the so-called "barotropic transport" that cannot be identified with only hydrography over the upper 2 km and the thermal or gradient wind relation. Therefore, Gulf Stream transport

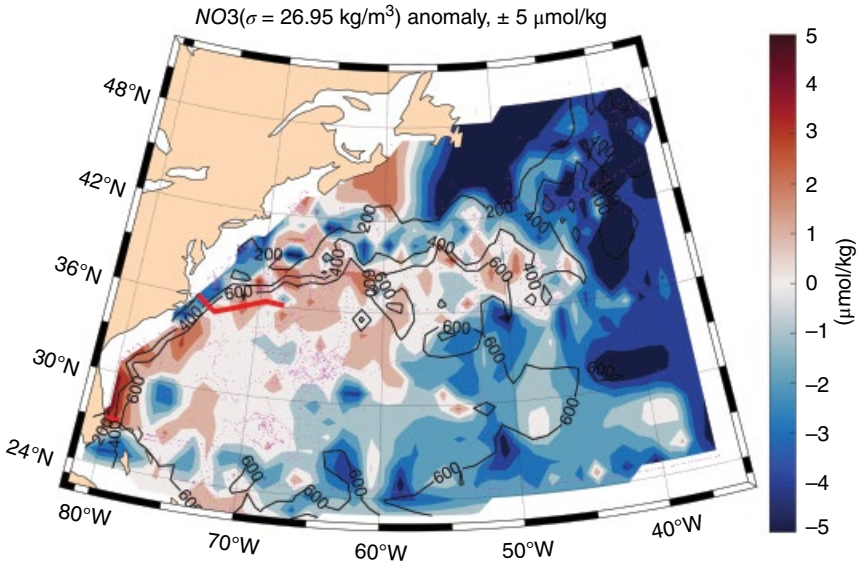

Figure 4.1 Nitrate NO_3^- on the $\sigma_\theta = 26.95\,\text{kg/m}^3$ potential density surface, plotted as an anomaly relative to the median, 16.4 µmol/kg. The depth of the potential density surface (in meters) is contoured. Gridded maps are constructed using triangle-based cubic interpolation using data from both the World Ocean Database (WOD13) (Boyer et al., 2013) and the biogeochemical argo array up to December 2017 (Johnson et al., 2013, 2017). Outliers, which are defined to be outside the central 95% quantile of the all the data in the region shown, are excluded. However, before removing outliers, there are 3774 profiles in total, 1219 of which are from argo floats (collected between 2009 and 2017) and all of which are collected between 1928 and 2017. Hydrographic sections shown in Figure 4.2 are plotted in red. Magenta dots indicate where relevant measurements were made. (*See insert for color representation of this figure*.)

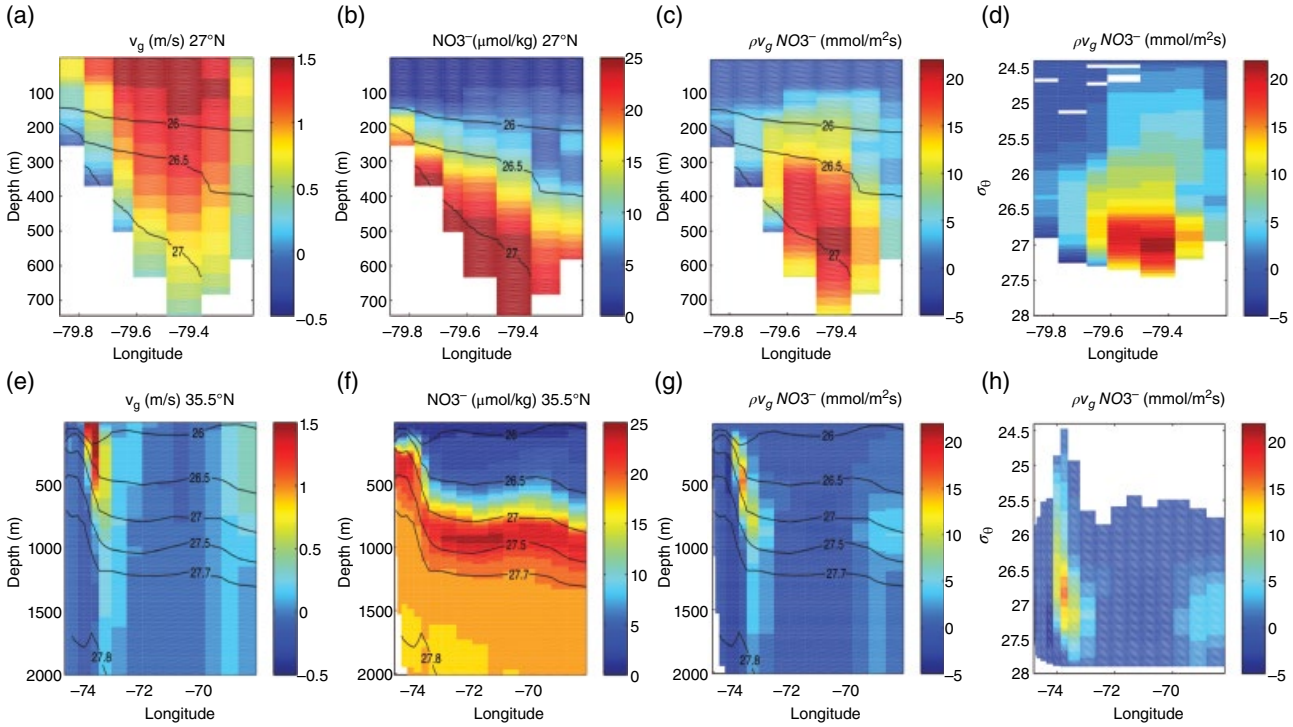

Figure 4.2 Data from two hydrographic sections across the Gulf Stream, including geostrophic velocity (with barotropic transport included) v_g in m/s ((a) and (e)), nitrate NO_3^- in µmol/kg ((b) and (f)), and nitrate flux $\rho v_g NO_3^-$ in mmol/(s m^2) as a function of depth ((c) and (g)) and potential density σ_θ ((d) and (h)). The section at 27° N crosses the Straits of Florida at 79.5° W ((a)–(d)) and the section at 35.5° N is just east of Cape Hatteras at 74° W ((e)–(h)); the sections are plotted in Figure 4.1. (Figure is modified from Williams et al., 2011.) (*See electronic version for color representation of this figure*.)

estimates derived from upper-ocean hydrographic data using the thermal wind relation are biased low.

4.2..2. Nutrient Concentrations and Transport Within the Gulf Stream

Nutrient concentrations vary significantly in and around the Gulf Stream. Hence, Gulf Stream nutrient transport is not trivially related to Gulf Stream volume transport. This section reviews observations of nutrient distributions in and around the Gulf Stream as well as associated observational estimates of Gulf Stream nutrient transport, which are derived from simultaneous observations of nutrient concentration, hydrography, and/or velocity. The section also includes a discussion of remaining points of uncertainty and disagreement about Gulf Stream nutrient transport in the literature.

4.2.2.1. Vertical and Horizontal Distribution of Nutrients

Cross-sections at various points along the Gulf Stream show that the concentrations of the macronutrients, including nitrate, phosphate, and silicate, are depleted at the surface, increase to a maximum in the upper 1 km but within the main pycnocline ($\sigma_\theta \approx 27.3\,kg/m^3$) and decrease slightly below that (Atkinson, 1985; Pelegrí & Csanady, 1991; Williams et al., 2011) (Figure 4.2f). In the main pycnocline, isopleths of nutrient are approximately aligned with isopycnals throughout much of the world's oceans (While & Haines, 2010; Omand & Mahadevan, 2013). The same is true in the Gulf Stream; isopycnals and isopleths of nutrient are aligned and both slope steeply across the stream (Figures 4.2b, 4.2f). Hence, vertical nutrient profiles in the separated Gulf Stream exhibit a nutrient-density relationship that is similar to the Slope Sea to the north and Sargasso Sea to the south, but a nutrient-depth relationship that is different from either (Figures 4.2 and 4.3).

Pelegrí and Csanady (1991), Reid (1994), and Palter and Lozier (2008) all show that the Gulf Stream is associated with slightly higher nutrient concentrations than the Slope Sea or Sargasso Sea waters to either side on isopycnals in the upper-pycnocline, i.e., $\sigma_\theta = 26.5$– $27.3\,kg/m^3$. These nutrient anomalies on isopycnals in the Gulf Stream are small in magnitude compared to the variations of nutrient with depth or across isopycnals, but they are a robust feature of the mean nutrient distribution on these isopycnals in the North Atlantic. To add more support for this last point, I present a map of nitrate anomaly on the $\sigma_\theta = 26.95\,kg/m^3$ isopycnal, which synthesizes observations from the 2013 World Ocean Database and over 1000 profiles from biogeochemical Argo floats and reveals enhanced nitrate along the entire path of the Gulf Stream, from the Straits of Florida to the Grand Banks (Figure 4.1). A negative nitrate anomaly at 25° N, 79° W in Figure 4.1 conflicts with the idea that the Gulf

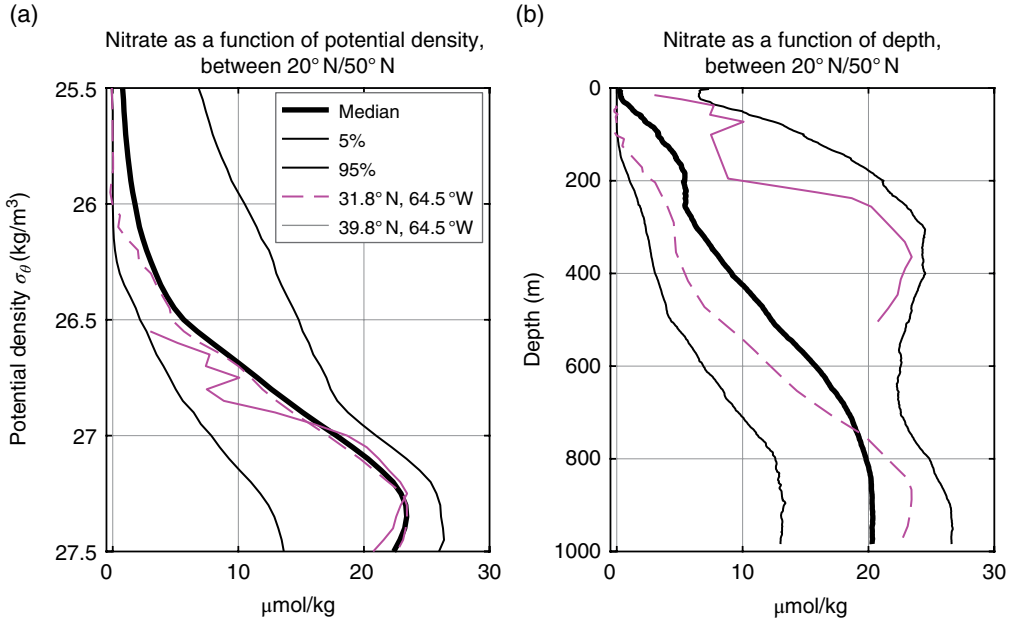

Figure 4.3 Distribution of nitrate as a function of potential density (a) and depth (b) in the North Atlantic. Magenta lines show two example profiles, one in the slope water to the northwest of the Gulf Stream in early March and one in the Sargasso Sea to the southeast of the Gulf Stream in late summer. The two example profiles differ markedly as a function of the depth coordinate, but collapse to nearly a single curve in the potential density coordinate. Data are the same as those used in Figure 4.1. (*See electronic version for color representation of this figure.*)

Stream has higher nutrient concentrations on isopycnals. However, this particular anomaly is based on less than 10 data points, as indicated by magenta dots in Figure 4.1. Therefore, I view this negative anomaly as very uncertain compared to positive anomalies elsewhere in the Gulf Stream that are based on many more observations.

4.2.2.2. Observational Estimates of Gulf Stream Nutrient Transport

The Gulf Stream transports nutrients along its path. Pelegrí and Csanady (1991) quantify this transport using a series of hydrographic sections with simultaneous measurements of nitrate, phosphate, and silicate concentrations over the top 2 km. They use the thermal wind relation to obtain a geostrophic velocity and the associated nutrient transports assuming no flow at 2 km depth. Later estimates of the Gulf Stream nutrient transport by Williams et al. (2011) are based on different observations but are qualitatively and quantitatively similar to the estimates of Pelegrí and Csanady (1991) in several ways. Both find that the streamwise advective flux is strongest over depths ranging from about 300 to 700 m and from $\sigma_\theta = 26.5$–$27.3\,\mathrm{kg/m^3}$ at both the Straits of Florida and just to the east of Cape Hatteras (as shown in Figures 4.2c, 4.2d, 4.2 g, and 4.2 h). Both also find that the Gulf Stream nutrient transport increases significantly from the Straits of Florida to Cape Hatteras, in conjunction with roughly comparable increases in volume transport (Figure 4.4). For example, the nitrate transport above $\sigma_\theta = 27.5\,\mathrm{kg/m^3}$ increases from about 300 kmol/s at the Straits of Florida to about 700–800 kmol/s just east of Hatteras, while the analogous volume transport increases from about 30 Sv to 80 Sv ($1\,\mathrm{Sv} = 10^6\,\mathrm{m^3/s}$).

4.2.2.3. Remaining Uncertainty and Disagreements in the Literature

There are some differences between the various published descriptions of the nutrient flux in the Gulf Stream. For example, perhaps because they assume a level of no motion at 2 km and integrate the thermal wind relation, the estimates of the integrated volume transport from 0 to 2 km depth in Pelegrí and Csanady (1991) are lower by 20 Sv or more in the sections crossing the separated Gulf Stream east of Cape Hatteras than in papers where the Gulf Stream transport in the top 2 km at this location is estimated using direct measurements of velocity. In particular, Pelegrí and Csanady (1991) report a volume transport of about 65–70 Sv in the top 2 km compared to estimates of 70–100 Sv obtained via direct velocity measurement between 73° W and 68° W (Halkin & Rossby, 1985; Hogg, 1992; Johns et al., 1995; Williams et al., 2011). The volume transport deficit between the observations of Pelegrí and Csanady (1991) and the others is approximately consistent with estimates for the "barotropic" component of the volume transport omitted by Pelegrí and Csanady (1991) due to the absence of deep velocity measurements for use as a bottom boundary condition for the thermal wind relation. Therefore, although Pelegrí and Csanady (1991) show that the baroclinic volume transport in the top 2 km remains approximately constant between 68° W and 53° W, studies have shown that the barotropic component of the transport in the top 2 km, and hence the total volume transport above 2 km depth, increases significantly between 68° W and 60° W (Hogg, 1992) due to convergence of eddy-related momentum fluxes (Waterman & Jayne, 2012; Waterman & Hoskins, 2013). In addition, since the

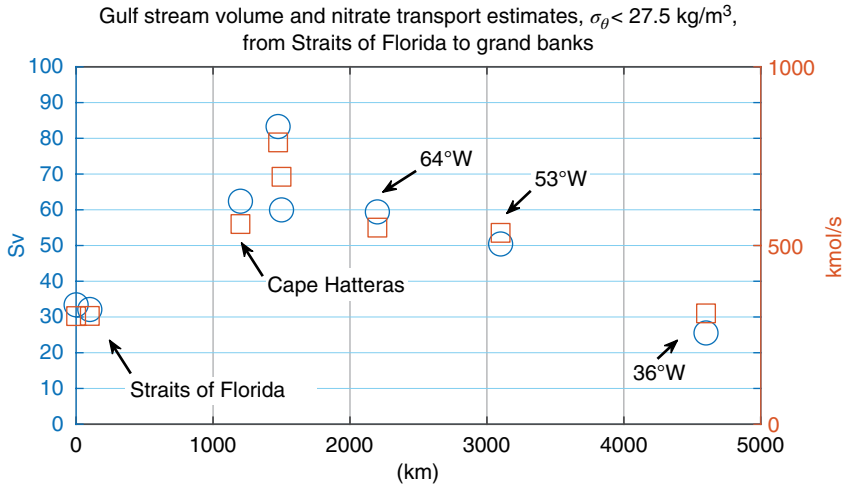

Figure 4.4 Gulf Stream volume and nitrate transports for $\sigma_\theta < 27.5\,\mathrm{kg/m^3}$ as a function of streamwise distance from the Straits of Florida. Data combined from Table 2 of Pelegrí and Csanady (1991) and Table 1 of Williams et al. (2011). Red squares indicate nitrate transport (right axis), whereas blue circles indicate volume transport (left axis). (*See electronic version for color representation of this figure.*)

nutrient transport is calculated by integrating volume transport times nutrient concentration over a Gulf Stream cross-section, it seems likely that the total nutrient transport in the upper 2 km also increases somewhat between Cape Hatteras and 64° W in the separated Gulf Stream (contrary to what is shown in Figure 4.4).

In addition, the observations of Pelegrí and Csanady (1991) differ from more recent hydrographic observations by Williams et al. (2011) in that the former show that the transport-weighted mean nitrate concentration on isopycnals increases above $\sigma_\theta = 26.8\,kg/m^3$ from the Straits of Florida to Cape Hatteras and decreases below, whereas the hydrographic sections used by Williams et al. (2011) show a decrease in the transport-weighted mean nitrate concentration above and below $\sigma_\theta = 26.8\,kg/m^3$. In my opinion, these differences likely reflect dynamical variability in both the volume transport and nutrient concentrations on isopycnals. A new estimate of the variability associated with the nutrient or volume transport on an isopycnal layer in the Gulf Stream can be obtained by comparing the hydrographic data in Pelegrí and Csanady (1991) and Williams et al. (2011), that is by comparing the results in their respective Table 4.1's. Although Williams et al. (2011) present data from two sections near Cape Hatteras, the section labeled 35.5° N, 74° W is used for comparison and only nitrate fluxes are discussed here. The comparison reveals a median coefficient of variation of 18% for Gulf Stream nitrate transport on six isopycnal layers. Here, the coefficient of variation is defined by $\sqrt{2}|T_W - T_P|/(T_W + T_P)$, where T_W is an estimate from Williams et al. (2011) and T_P is an estimate from Pelegrí and Csanady (1991) and the six isopycnal layers are defined by: $\sigma_\theta < 26.2\,kg/m^3$, $26.5 > \sigma_\theta > 26.2\,kg/m^3$, $26.8 > \sigma_\theta > 26.5\,kg/m^3$, $27.1 > \sigma_\theta > 26.8\,kg/m^3$, $27.3 > \sigma_\theta > 27.1\,kg/m^3$, and $27.5 > \sigma_\theta > 27.3\,kg/m^3$. The differences $T_W - T_P$ take both signs, which suggests that a barotropic transport offset cannot account for all the differences between the two sections. This estimated coefficient of variation for nitrate transport is consistent with the estimated 20% coefficient of variation for volume transport at 73° W derived from sustained velocity observations (Halkin & Rossby, 1985). In addition, Pelegrí et al. (2006) obtain a similar estimate for the coefficient of variation of the nitrate transport by using a fixed nitrate/potential temperature relationship and estimating the variations in nitrate transport using sustained observations of velocity and temperature first discussed by Halkin and Rossby (1985).

Another perspective is provided by Palter and Lozier (2008), who show that the profiles in the 2005 World Ocean Database show a decrease in phosphate concentration along the stream on isopycnals $\sigma_\theta > 26.5\,kg/m^3$, although the effect is relatively small compared to the variability, especially for $26.5 < \sigma_\theta < 27.0\,kg/m^3$ (see Table 1 of Palter & Lozier, 2008). Likewise, the map of nitrate concentration on $\sigma_\theta = 26.95\,kg/m^3$ in Figure 4.1 shows a slightly decreasing nitrate concentration from the Straits of Florida to Cape Hatteras (i.e., 27–36° N). On the other hand, the nitrate concentration increases again to the east of Cape Hatteras in the separated Gulf Stream and remains elevated compared to the Slope Sea and Sargasso Sea out to about 50° W. This observation is also qualitatively consistent with the results of Palter and Lozier (2008), who observed a slight eastward increase in the phosphate concentration on the $\sigma_\theta = 26.9\,kg/m^3$ isopycnal in four hydrographic sections across the separated Gulf Stream (see Palter & Lozier, 2008, Figure 11). However, any attempt to quantitatively constrain the along-stream isopycnal nutrient gradients to be different from zero should be viewed as rather uncertain due to the limited data in this region (~500 profiles distributed unevenly in time and space over the last 70 years), although the data may be sufficient for formal statistical significance in some parts of the stream, especially on deeper isopycnals (Palter & Lozier, 2008).

4.2.3. Sources and Sinks of Gulf Stream Nutrients

Two hypotheses have been proposed to explain the source of enhanced nutrient concentrations on upper-pycnocline isopycnals ($\sigma_\theta = 26.5$– $27.3\,kg/m^3$) in the Gulf Stream. First, since nutrient concentrations are higher on upper-pycnocline isopycnals in the tropics (Reid, 1994) and a substantial fraction of the water flowing through the Straits of Florida is of tropical origin (Schmitz & Richardson, 1991), the inflow of tropical nutrients along the upper limb of the AMOC is a plausible cause for the enhanced nutrient concentrations (Palter & Lozier, 2008). Simulations of the Atlantic basin by Williams et al. (2006, 2011) largely support this view; they show that a significant fraction of the water and nutrients passing through the Florida Straits originates in the Southern Hemisphere. Furthermore, observations of the ratios of different nutrient concentrations and global model simulations suggest that the subantarctic mode water in the Southern Ocean represents an important source of Gulf Stream nutrients in the pycnocline (Sarmiento et al., 2004). In support of this hypothesis, idealized simulations of an Atlantic basin coupled to a re-entrant Southern Ocean channel show that winds in the Southern Ocean can remotely impact biogeochemistry in the subpolar North Atlantic by modifying the AMOC, which passes through the Gulf Stream (Bronselaer et al., 2016).

However, nutrient concentrations on isopycnals along the stream also receive a boost from diapycnal mixing, as suggested by Pelegrí and Csanady (1991, 1994) and Jenkins and Doney (2004) and are also diluted by isopycnal mixing, as suggested by Palter and Lozier (2008) and Williams et al. (2011). However, the contribution of

biological processes to the along-stream evolution of the nutrient concentration on isopycnals below the well-lit euphotic layer is thought to be negligibly small, since the transit time between the Straits of Florida and the Grand Banks (i.e., about 34–17 days to cover 3000 km at 1–2 m/s) is relatively short compared to biological remineralization timescales (Palter & Lozier, 2008). But, how strong is the plausible source of nutrients along the Gulf Stream path due to diapycnal mixing, and how does this compare with losses along the Gulf Stream path due to isopycnal mixing?

The timescales associated with turbulent diapycnal and isopycnal diffusion in the Gulf Stream are indicative of how important each process is for maintaining and destroying the nutrient concentration anomaly in the Gulf Stream nutricline. For example, the timescale associated with diapycnal diffusion $\Delta H^2/\kappa_\rho$ where the vertical depth scale of the nutricline $\Delta H \approx 100-300$ m (Figures 4.2 and 4.3) and the turbulent diapycnal diffusivity of nutrient $\kappa_\rho \approx 10^{-5}$–$10^{-4}$ m^2/s (e.g., Table 4.1) is of the order of 10^3–10^4 days. Even if the diffusive timescales are scaled down by a factor of 2–10, because the ratio of the nutrient change across isopycnals in the nutricline (e.g., 10–20 mmol/m^3 nitrate) to the nutrient anomaly on isopycnals (e.g., 2–5 mmol/m^3 nitrate) is about 2–10, the diffusive timescales are still one to two orders of magnitude longer than the advective timescale from the Straits of Florida to the Grand Banks, which is only a few weeks. Hence, diapycnal mixing is too slow to significantly contribute to the nutrient anomalies on upper-pycnocline isopycnals of the Gulf Stream. On the other hand, the timescale associated with isopycnal mixing is $\Delta L^2/\kappa_H$, where $\kappa_H \sim 10^2$–10^4 m^2/s is an effective isopycnal diffusivity (Bower et al., 1985; Joyce et al., 2013a; Klocker & Abernathey, 2014), and the horizontal length scale $\Delta L \approx 5$–10×10^4 m is the characteristic half-width the Gulf Stream. This scaling yields a minimum timescale of a few days, which is sufficiently short to potentially explain the disappearance of the Gulf Stream nutrient anomaly near the Grand Banks (Figure 4.1). However, the nutrient anomaly in the Gulf Stream persists from the Straits of Florida to the Grand Banks, over an advective timescale of weeks with relatively small time-mean streamwise gradient; this suggests that the effective cross-stream isopycnal diffusivity is at least an order of magnitude smaller than 10^4 m^2/s in most places along the Gulf Stream path. A complimentary and supporting measure of the isopycnal diffusive timescale can be derived from the characteristic residence time of the isopycnal RAFOS floats deployed in the main pycnocline of the separated Gulf Stream, which is about three weeks (Bower & Rossby, 1989) and suggests an isopycnal diffusivity $\kappa_H \sim 10^3$ m^2/s. Further discussion of the contributions of diapycnal and isopycnal mixing to the Gulf Stream nutrient budget and a table of relevant results from the literature can be found in section 3.3 of Palter & Lozier (2008).

4.2.4. Fate of Gulf Stream Nutrients

Near the Grand Banks (50° W), the Gulf Stream breaks apart in a region of very energetic mesoscale variability and a complex mean flow structure (Krauss, 1986; Rossby, 1996; Carr & Rossby, 2001; Mertens et al., 2014), which is thought to be an important source of variability in the AMOC and inter-gyre exchange (Buckley & Marshall, 2016). How much of the Gulf Stream's nutrients flow into the subpolar and subtropical gyres on each isopycnal? How does the Gulf Stream nutrient stream contribute to setting the mean nutrient concentration on isopycnals and in the surface mixed layer in the subtropical and subpolar gyres? Pelegrí et al. (1996, 2006) point to a tongue of enhanced surface nitrate extending from the Grand Banks toward Iceland in the nutrient maps of Reid (1994) as evidence that a significant fraction of the Gulf Stream nutrients reach the middle of the subpolar gyre in the North Atlantic via isopycnal advection from the Gulf Stream into the North Atlantic Current and ultimately enter the mixed layer. A schematic from Williams et al. (2006) illustrates how the nutrient is advected from the Gulf Stream to the subpolar gyre (Figure 4.5a): nutrients are transported along the Gulf Stream on sloping isopycnals until they reach the surface mixed layer via advection or entrainment. Hence, the location where the Gulf Stream nutrients enter the mixed layer depends significantly on the potential density/depth of the associated water in the Gulf Stream (Burkholder & Lozier, 2014). In the mixed layer, a large fraction of the poleward flowing inorganic nutrient is converted into organic form via photosynthesis and either subducted into the subtropical gyre in dissolved organic form (Rintoul & Wunsch, 1991) or transformed to denser water via sinking organic particles or heat loss to the atmosphere.

Another major fraction of the poleward flowing inorganic nutrient in the mixed layer is transformed to denser water without passing through organic form via surface heat loss. Several rather crude but consistent observational metrics support this view. First, observations of surface drifter trajectories suggest that there is little exchange of water via surface pathways from the subtropical to the subpolar gyre (Brambilla & Talley, 2006; Hakkinen & Rhines, 2009), whereas the majority of Lagranian drifters (with a fixed specific volume) on deep isopycnals $\sigma_\theta > 27.2$ kg/m^3 apparently pass from the subtropical into the subpolar gyre along the North Atlantic Current. However, the latter point is more obvious in models (Williams et al., 2006; Burkholder & Lozier, 2011, 2014) than in observations (Rossby, 1996; Carr & Rossby,

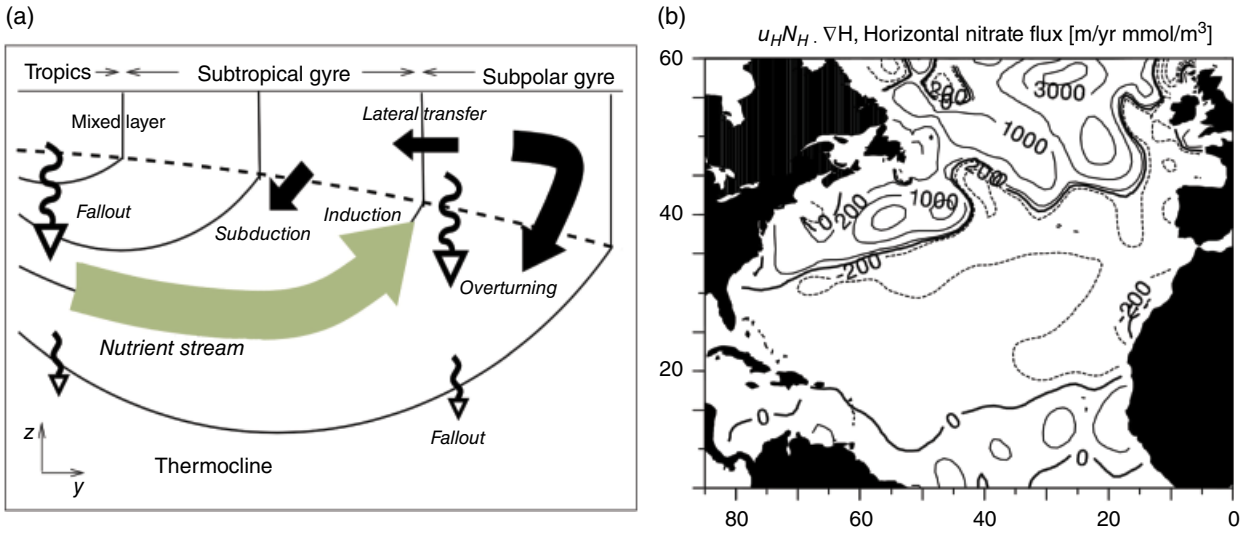

Figure 4.5 (a) The fate of the Gulf Stream nutrient stream: induction into the mixed layer at the northern margin of the subtropical gyre or in the subpolar gyre and (b) an estimate of the (dominant) horizontal component of the climatological nitrate induction flux based on winter mixed layer depths H, the geostrophic velocities at these depths $\mathbf{u}_H$, and nitrate concentrations at these depths N_H, all from the World Ocean Database. (Reproduced from Williams et al., 2006.)

2001) due to the limited number and duration of such isopycnal drifter deployments. Second, the inverse model of Rintoul and Wunsch (1991) (based on one transatlantic section) shows that there is a net northward nitrate transport of about 350 kmol/s above $\sigma_\theta = 27.5\,\text{kg/m}^3$ at 36° N, which is about half the estimated Gulf Stream nitrate transport at this latitude and about equal to the flow of nitrate through the Straits of Florida (Figure 4.4). In contrast, the zonally-integrated northward volume flux above $\sigma_\theta = 27.5\,\text{kg/m}^3$ at 36° N, about 15 Sv, is about half the flux through the Straits of Florida, which suggests that a significant fraction of the southward flowing water in the upper-ocean gyre circulation has been ventilated and stripped of its inorganic nutrients before being subducted back into the subtropical gyre. Third, the northeastward nitrate transport on isopycnals $\sigma_\theta < 27.5\,\text{kg/m}^3$ drops from about 690 kmol/s at 70° W to 310 kmol/s at 35° W in the hydrographic sections analyzed by Pelegrí and Csanady (1991). This zonal flux convergence suggests local biological consumption and/or northward transport in the North Atlantic Current of about 380 kmol/s, although a significant fraction of this reduction in nutrient flux is probably associated with detrainment of Gulf Stream water and nutrients into recirculation gyres that ultimately feed back into the stream. Finally, Williams et al. (2006) use the World Ocean Database to estimate the climatological Eulerian-mean induction flux of nitrate into the surface mixed layer, that is the advection of nitrate along isopycnals into the surface mixed layer (Figure 4.5). The estimated induction flux for $\sigma_\theta < 27.5\,\text{kg/m}^3$ is 288 kmol/s, which is roughly consistent with the 350 kmol/s net northeastward nitrate flux at 36° N as quantified by Rintoul and Wunsch (1991) and the 380 kmol/s zonal advective flux convergence of nitrate between 70° W and 35° W, as quantified by Pelegrí and Csanady (1991).

All these observational results suggest that surface waters that have been stripped of their nutrients near the gyre boundary mostly do not flow northward to replace the surface waters of subpolar gyre lost via water mass transformation to deep convection. Rather, the waters that replenish the surface layer of the subpolar gyre are mostly from deeper depths in the Gulf Stream or North Atlantic Current and are therefore nutrient rich. In addition, these results support the hypothesis that the northward ispopycnal advective flux of nutrients is the dominant source of nutrients to lighter isopycnals $\sigma_\theta < 27.5\,\text{kg/m}^3$ in the subpolar North Atlantic. Hence, the magnitude of the northward advective flux of nutrients in the Gulf Stream is an important constraint on the export flux of organic nutrients to the abyssal ocean in the subpolar gyre on interannual and longer timescales. However, there is considerably more uncertainty about both the spatial and temporal variability of the sink of Gulf Stream nutrients, via induction and biological consumption or recirculation, than there is about the nutrient transport along the Gulf Stream path from the Straits of Florida to the Grand Banks; the complex dynamics where the Gulf Stream breaks apart near the Grand Banks and the spatially diffuse nature of the sink are two leading causes of this uncertainty.

4.2.5. Summary

The Gulf Stream is a nutrient stream. About 30 Sv of water and 300 kmol/s of nitrate flow through the Straits of Florida above the $\sigma_\theta = 27.5\,kg/m^3$ isopycnal, and comparably large fluxes of phosphate and silicate are also observed (Pelegrí & Csanady, 1991; Williams et al., 2011). As water from the Sargasso Sea enters the Gulf Stream, the volume and nutrient transport increase approximately proportionally; both approximately double before reaching Cape Hatteras and then increase by about 30% further downstream of the separation point. The observed correlation between changes in volume and nutrient transport (Figure 4.4) supports the hypothesis that the increases in nutrient transport along the stream are driven primarily by isopycnal (i.e., adiabatic) entrainment of nutrient-rich pycnocline water from the Sargasso Sea and the Slope Sea into the Gulf Stream. Despite the large volume of recirculating water in the Gulf Stream, the data support the hypothesis that nutrients are elevated on upper-pycnocline isopycnals along the Gulf Stream path from the Straits of Florida to the Grand Banks compared to the Sargasso Sea or the Slope Sea (Figure 4.1). Analysis supports the hypothesis that the dominant source of the water with elevated nutrient concentrations is an isopycnal pathway from the tropics and, ultimately, the Southern Hemisphere, and that biological remineralization, diapycnal mixing and isopycnal mixing do not significantly modify these concentrations along most of the Gulf Stream path due to their relatively long timescales compared to the advective timescale for upper-pycnocline water to transit from the Straits of Florida to the Grand Banks (as little as a few weeks). The fate of Gulf Stream nutrients past the Grand Banks is not very well constrained by observations, but multiple crude estimates suggest that about half of the nutrients end up irrigating the surface waters of the subpolar gyre and sustaining primary and export production there, whereas the other half irrigates the intergyre boundary and is subducted or recirculated into the subtropical gyre (Pelegrí & Csanady, 1991; Rintoul & Wunsch, 1991; Pelegrí et al., 1996, 2006; Williams et al., 2006).

4.3. PROJECTED DECLINE OF GULF STREAM NUTRIENT FLUX IN SIMULATIONS WITH CESM

Observations and model results suggest that the Gulf Stream nutrient transport, as a part of the upper limb of the meridional overturning circulation, is a crucial component in global biogeochemical cycles, and hence the Earth system, like the Gulf Stream heat transport. In addition, the Gulf Stream nutrient transport may play a crucial role in the forced Earth system response to anthropogenic emissions during the 21st century. However, previous studies have not quantified how the Gulf Stream nutrient transport is expected to evolve in Earth system model projections for the 21st century. Yet, previous studies have shown that Earth system models project significant and robust declines in surface nitrate, phytoplankton primary production, phytoplankton and higher trophic level biomass (including fish), and export of organic material to the deep ocean in the subpolar North Atlantic during the 21st century in the RCP8.5 emissions scenario (Frölicher et al., 2009; Steinacher et al., 2010; Marinov et al., 2010, 2013; Bopp et al., 2013; Dutkiewicz et al., 2013; Moore et al., 2013; Krumhardt et al., 2017; Stock et al., 2017). These reductions are of interest because the subpolar North Atlantic is characterized by a dramatic spring phytoplankton bloom with high phytoplankton concentrations and significant export of organic material to depth in the present climate (Behrenfeld & Boss, 2014; Siegel et al., 2014). Therefore, changes in the subpolar North Atlantic have global as well as regional biogeochemical and ecological implications. Although the physical mechanisms driving these biogeochemical declines have not been fully explored, they are thought to be driven primarily by a reduction in the supply of nutrient to the euphotic layer due to a reduction in deep mixing associated with enhanced upper-ocean stratification and/or a reduction in the AMOC (Schmittner, 2005; Frölicher et al., 2009; Steinacher et al., 2010; Doney et al., 2012), which may be associated with reductions in Gulf Stream transport.

However, the links between the Gulf Stream transport and AMOC are not fully understood (Yeager, 2015; Buckley & Marshall, 2016). Buckley and Marshall (2016) review a few relevant and robust results about interannual to decadal AMOC variability. For example, observations and models have shown that AMOC variability tends to be meridionally incoherent between the subtropical and subpolar gyre on interannual timescales but meridionally coherent on decadal and longer timescales. For several reasons, upper-ocean buoyancy anomalies along the western boundary, which first appear either near the subtropical–subpolar gyre boundary or in the subpolar gyre, are a precursor for meridionally coherent AMOC anomalies in the subtropical and subpolar North Atlantic. However, there are a multitude of mechanisms that can create these buoyancy anomalies or communicate the associated signal meridionally. For example, changes in the wind-driven and eddy-driven gyre circulations may play a role in the creation or communication of buoyancy anomalies on the western boundary and in inducing meridionally coherent AMOC anomalies. Analysis of the barotropic vorticity dynamics in CESM by Yeager (2015) highlights various connections between gyre circulations and AMOC. In the subpolar gyre, there is a strong correlation between anomalies in the gyre

circulation and AMOC on decadal timescales because the bottom pressure torque is the dominant term in the barotropic vorticity budget. Hence, decadal variations in air–sea buoyancy forcing, which drive variations in the bottom pressure torque in the presence of variable topography, drive variations in the coupled subpolar gyre/AMOC circulation. In addition, since the bottom pressure torque is a dominant term in the barotropic vorticity balance near the subtropical–subpolar gyre boundary, changes in the buoyancy-driven AMOC, deep boundary currents, and thereby the bottom pressure torque, can influence the Gulf Stream above. Finally, negative anomalies of wind-driven vorticity input at the surface of the subtropical gyre (associated with spin up of the anticyclonic wind-driven gyre and the Gulf Stream) are balanced by positive anomalies in bottom pressure torque in the abyssal ocean that are associated with spin down of AMOC.

Hence, Gulf Stream transport, which includes the eddy-driven and wind-driven gyre circulations, is nonlinearly and nontrivially coupled to AMOC transport both locally in the subtropics and remotely at all other latitudes. Nevertheless, the hypothesis supported by the results presented below is that multidecadal, forced changes in AMOC during the 21st century of the RCP8.5 emissions scenario are dominated by a meridionally coherent AMOC response in the North Atlantic and, in particular, are associated with reductions in the part of AMOC passing through the Gulf Stream. The results presented below quantify the forced reductions in both AMOC and Gulf Stream fluxes of volume and nitrate from 2006 to 2080 in the RCP8.5 emissions scenario using a large ensemble of simulations with CESM. In addition, comparisons are made between the forced reductions in these advective nitrate fluxes and the forced reductions in the entrainment and export fluxes in the subpolar gyre, which are associated the seasonal cycle of mixing and restratification and with sinking particulate organic nitrogen respectively.

Based on the scalings presented in the introduction, significant multidecadal forced changes in the transport of nutrient in the AMOC are likely to drive equally large percentage changes in the net nutrient flux to upper ocean isopycnals $\sigma_\theta < 27.5\,\mathrm{kg/m^3}$ in the subpolar North Atlantic. This hypothesis has an analogue for heat transport, which posits a strong correlation between changes in the AMOC and changes in upper ocean heat content in the subpolar North Atlantic; stronger reductions in the AMOC are associated with less North Atlantic warming in simulations with increasing CO2 (Winton et al., 2014). Here, it is hypothesized that the anthropogenically-forced reduction in the upper limb of the AMOC (Weaver et al., 2012; Cheng et al., 2013), which has a significant fingerprint on the Gulf Stream transport, is a dominant driver of the anthropogenically forced reduction in the supply of nutrient to the surface mixed layer in the subpolar North Atlantic (in addition to changes in vertical mixing and entrainment associated with enhanced upper ocean stratification that is often cited, including in the context of CESM (Moore et al., 2013)). Therefore, the forced reduction in AMOC is an important driver of the anthropogenically forced reduction in new primary production and the associated export of organic material to the deep ocean in the North Atlantic subpolar gyre of Earth system models. This hypothesis is implicitly supported by the observational analysis of Barton et al. (2015) in the subpolar North Atlantic, which shows that although local physical processes (e.g., surface mixing) have a strong influence on phytoplankton communities on shorter timescales, such as during the seasonal cycle, other factors, such as ecosystem dynamics (Beaugrand et al., 2002; Edwards & Richardson, 2004; Sommer & Lewandowska, 2011; Behrenfeld & Boss, 2014) and variations in the AMOC and gyre circulations, are important drivers of interannual to multidecadal variability in phytoplankton communities. However, the relative strength of the seasonal oscillation of plankton and biogeochemical constituents in the subpolar North Atlantic makes it challenging (particularly observationally) to study variability on longer timescales, which has a relatively small amplitude compared to the seasonal oscillation (Palevsky & Nicholson, 2018).

4.3.1. Model Description

Here, some features of the Gulf Stream nutrient stream relevant to this hypothesis are explored using a 34-member subset of a large (40 member) ensemble of fully-coupled simulations of the period from 1920 to 2100 with the Community Earth System Model version 1 (CESM1) with online ocean biogeochemistry, which are generated from a single run by perturbing the atmospheric state with a very small amount of noise at 1920 (Kay et al., 2015). The ocean component of CESM1 is the parallel ocean program (Smith et al., 2010) configured with a nominal 1° horizontal resolution with refinement in the meridional direction near the equator, and 60 vertical levels with 10 m grid spacing over the top 150 m and a stretched grid below 150 m with spacings that range from 10 m at 150 m to 250 m at the ocean bottom. The ocean Biogeochemistry Elemental Cycling component output of the CESM1 solutions has been discussed and compared to observations (Moore et al., 2013; Long et al., 2013; Lindsay et al., 2014), and several previous papers have discussed the marine biogeochemical output in the large ensemble specifically (Long et al., 2016; Lovenduski et al., 2016; McKinley et al., 2016; Krumhardt et al., 2017). Although no previous study has explicitly discussed the evolution of the Gulf Stream nutrient stream in the 21st century in CESM1, Kim et al.

(2018) discuss the variability of the AMOC in the large ensemble and its relationship to variability in North Atlantic climate. The primary advantage of using an ensemble is that forced changes due to the emissions can be separated from unforced internal variability in the model, which eliminates one potential source of uncertainty in the model projections. Only 34 members (which are labeled 1–2, 9–35, 101–105 in the data archive on http://www.earthsystemgrid.org) are used here, because the biogeochemistry was corrupted in ensemble members 3–8. Using more members will not qualitatively change the results but will give a more precise separation between internal variability and the forced trend. No explicit comparisons are made with other Earth system models here, but other models are expected to yield qualitatively similar results. Danabasoglu et al. (2014) provide comparisons of the AMOC in CESM1 with other Earth system models in 20th century hind-cast experiments under CORE-2 historical atmospheric conditions, and Cheng et al. (2013) provide comparisons of AMOC between CMIP5-class Earth system models, which include CCSM4, a predecessor to CESM1 (some further discussion of this issue also appears in section 4.3.3 below).

4.3.2. Model Results

This section reports results from CESM1, which are summarized in Table 4.2, including the forced changes in Gulf Stream and AMOC volume and nitrate fluxes (section 4.3.2.1) between 2006 and 2080 as well as forced changes in entrainment and export fluxes in the subpolar North Atlantic over the same time period (section 4.3.2.2). The analysis focuses on the nitrate budget above $\sigma_\theta = 27.5\,\mathrm{kg/m^3}$. This bounding isopycnal is chosen because most of the northward flowing transport associated with AMOC lies above this isopycnal both in 2006 and 2080 (Figure 4.6) and it is at a relatively shallow depth of about 100–200 m but below the well-lit surface layer where phytoplankton grow (roughly the top 100 m) during summer. Finally, this isopycnal outcrops in the deep convection regions during winters of both 2006 and 2080, but the area where it outcrops declines significantly during this period. The results presented are qualitatively robust to small changes in this bounding isopycnal layer.

4.3.2.1. Forced Changes in the Subtropical North Atlantic Ocean Circulation and Associated Nitrate Fluxes between 2006 and 2080 in CESM

The AMOC volume transport declined by about 45% from about 23 Sv in 2006 to 13 Sv in 2080 at 40° N (Figure 4.6), which is within the 15–60% reduction observed in the AMOC over the 21st century in CMIP5 models (Cheng et al., 2013). In addition, Figure 4.6 shows that the reduction in AMOC volume transport between 2006 and 2080 is approximately proportional to a similar percentage reduction in zonally-integrated, ensemble-and-annual mean nitrate transport, from about 425 to 225 kmol/s over the same time period. Figure 4.7 highlights the meridional coherence of the forced reductions in AMOC volume and nitrate transport between 2006 and 2080 in CESM1. In particular, forced reductions in the poleward transport in the subtropical latitudes occur simultaneously with forced reductions in the poleward transport at subpolar latitudes over this time period. In addition, Figure 4.7 shows that although there is significant spread between the ensemble members, the forced reduction in zonally-integrated volume and nitrate transport for $\sigma_\theta < 27.5\,\mathrm{kg/m^3}$ is significantly larger than the spread between ensemble members. These reductions in the zonally-integrated northward nitrate and volume transport in the North Atlantic occur in conjunction with a slowing of the Gulf Stream and a reduction in the associated Gulf Stream nitrate flux in CESM1 (Figures 4.8 and 4.9). For example, the total eastward transport above $\sigma_\theta = 27.5\,\mathrm{kg/m^3}$ across a section from 35° to 45° N at 64° W declines by about 25% from about 37 Sv in 2006 to 28 Sv in 2080 (the interquartile ranges for the different ensemble members for this and other results are reported in Table 4.2). In addition, the corresponding nitrate transport along this section at 64°W declines by about 34% from about 534 kmol/s in 2006 to 352 kmol/s in 2080. Likewise, the total northward transport above $\sigma_\theta = 27.5\,\mathrm{kg/m^3}$ across a section out to 69° W at 30.5° N declines by about 22% from 38 Sv in 2006 to 29 Sv in 2080. In this 30.5° N section, the corresponding nitrate transport declines by about 34% from 518 kmol/s in 2006 to 339 kmol/s in 2080. The section maps in Figure 4.9 show that the reduction in nitrate transport is partially due to reductions in nitrate concentrations on isopycnals and partially due to reductions in volume transport. The percentage changes in nitrate concentration are smaller (~10%) compared to the percentage changes in volume and nitrate transport (~20–30%), which indicates that the forced change in Gulf Stream volume transport is the comparatively more important driver of the forced change in Gulf Stream nitrate transport. Finally, reductions in Gulf Stream volume and nitrate transport are comparable in magnitude to the reductions in the zonally-integrated volume and nitrate transport associated with AMOC in the North Atlantic (Table 4.2). Hence, most of the reduction in zonally-integrated transport in the subtropics can be accounted for by reductions in Gulf Stream transport (Figure 4.8).

4.3.2.2. Forced Changes in Entrainment and Export in CESM

In the RCP8.5 emissions scenario, forced changes in the zonally-integrated advective nitrate flux to the North

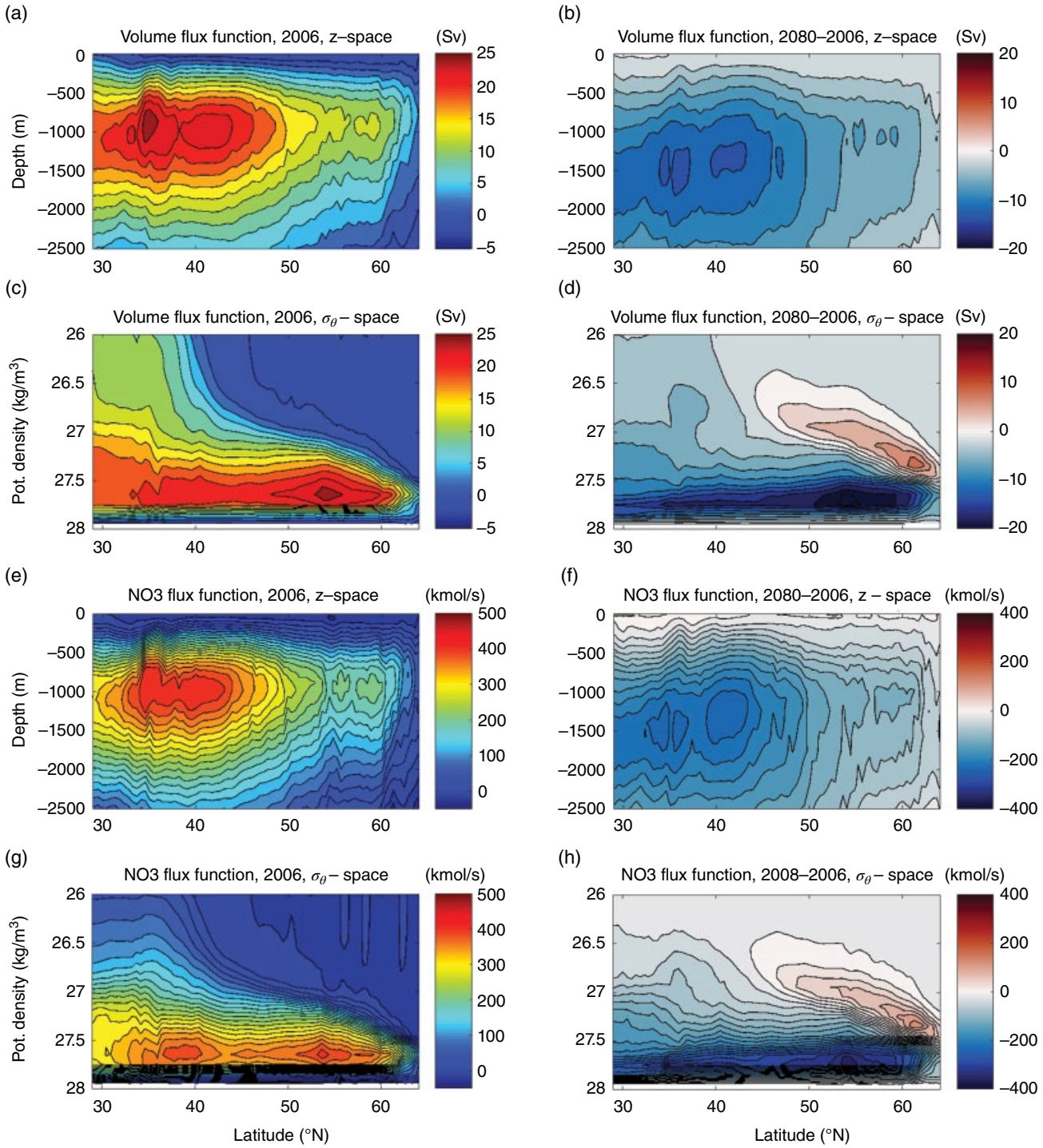

Figure 4.6 The zonally-integrated, annual-and-ensemble mean volume transport function (i.e. stream function) and nitrate transport function associated with the Atlantic meridional overturning circulation (AMOC) during 2006 as a function of depth ((a) and (e)) and density ((c) and (g)) from 34 ensemble members of the CESM1 large ensemble (Kay et al., 2015). Differences between 2080 and 2006 are shown in (b), (d), (f), and (h). Transports due to the parameterized eddy fluxes from the Gent and McWilliams (1990) and Fox-Kemper et al. (2011) parameterizations are a small contribution and omitted here. Contours are plotted every 2 Sv in (a)–(d) and 20 kmol/s in (E)–(H). (*See electronic version for color representation of this figure.*)

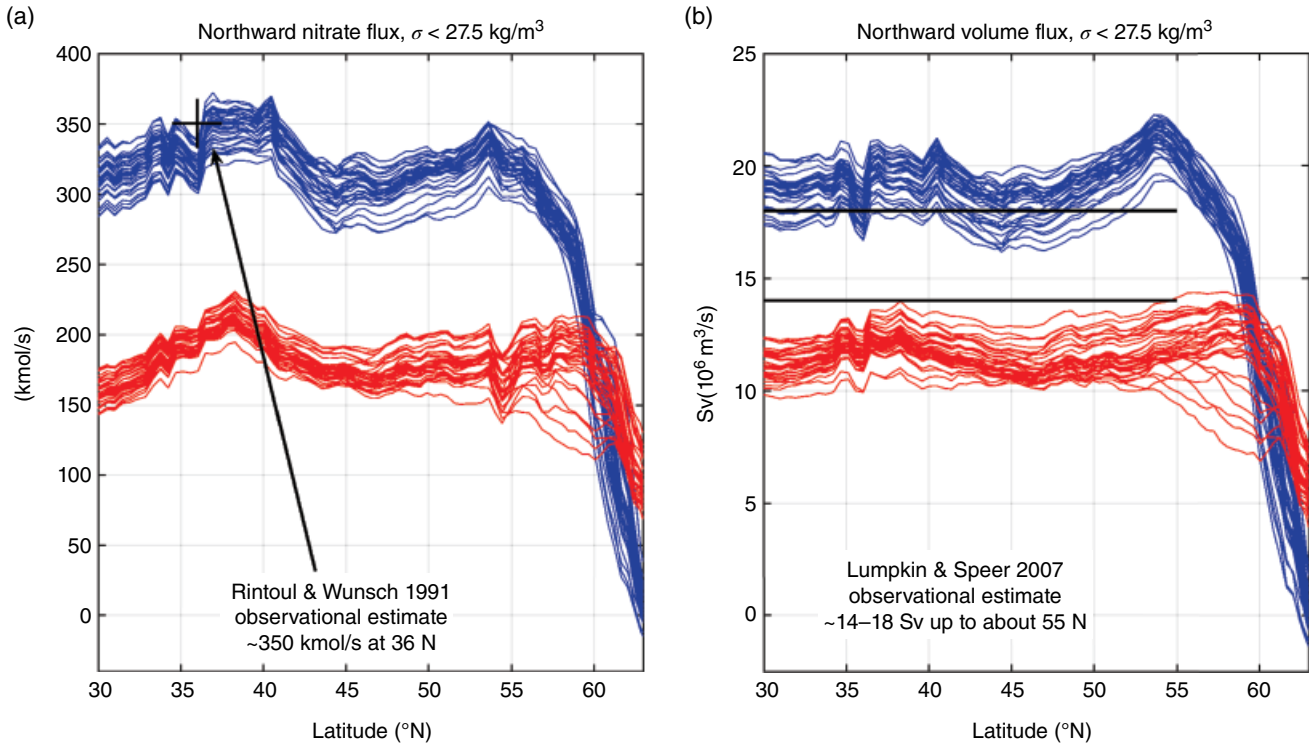

Figure 4.7 The zonally-integrated annual mean nitrate transport function (a) and volume flux function (i.e., streamfunction) (b) as in Figure 4.6, but summed over an isopycnal layer $\sigma_\theta < 27.5$. Different ensemble members are plotted as separate lines (2006 in blue = dark gray, and 2080 in red = light gray) to give a sense of the magnitude of the forced change relative to internal variability. The approximate location of the observations of Rintoul and Wunsch (1991) are noted by a black cross in (a); their observed net volume flux at 36 °N on these isopycnals is similar to Lumpkin and Speer (2007), which is noted by black lines in (b). (*See electronic version for color representation of this figure.*)

Atlantic subpolar gyre occur together with forced changes to other terms in the upper ocean nitrate budget of the subpolar gyre ($\sigma_\theta < 27.5\,kg/m^3$). Two other processes that are major contributors to this nitrate budget are the annual cycle of wintertime mixing and restratification and the export flux associated with the conversion of nitrate into new production and the subsequent export of organic nitrogen to denser water via sinking particles. In deep convection regions, the mixed layer seasonally becomes denser than $\sigma_\theta = 27.5\,kg/m^3$ during winter and subsequently restratifies during summer; this cycle induces an annually-averaged flux of nitrate from waters with $\sigma_\theta > 27.5\,kg/m^3$ to waters with $\sigma_\theta < 27.5\,kg/m^3$ (Williams et al., 2000). Conversely, the export flux of particulate organic nitrogen and subsequent remineralization in denser water induces an annually-averaged flux of nitrate from waters with $\sigma_\theta < 27.5\,kg/m^3$ to waters with $\sigma_\theta > 27.5\,kg/m^3$ (Buesseler & Boyd, 2009; Martin et al., 2011; Sanders et al., 2014). This section presents several different measures of the forced changes to the entrainment and export fluxes north of 48° N between 2006 and 2080 in CESM1, which can be compared with the forced changes in the northward advective nitrate flux discussed in the previous section.

The warming of the upper ocean during the 21st century drives a forced reduction in the area where $\sigma_\theta = 27.5\,kg/m^3$ outcrops during March and a forced reduction in the annual wintertime entrainment nitrate flux across this isopycnal and into the biologically active layer in the upper ocean (Figure 4.10). Here, entrainment is quantified from monthly mean outputs of the surface boundary layer thickness H_{BLT} (which is an actively mixing layer, as defined in Large et al., 1994), nitrate $NO3$, and density (defined from temperature and salinity). Similar to Williams et al. (2000), the rate of increase in nutrient in the biologically-active surface layer with thickness H_{BIO} that is associated with wintertime entrainment is approximated by:

$$F_{EN} = \frac{\partial H_{BLT}}{\partial t}\left(NO3_{PYC} - NO3_{BL}\right)\Lambda\frac{H_{BIO}}{H_{BLT}}$$

(For a derivation of the entrainment flux and some insight into the assumptions used here, see Whitt et al., 2017.)

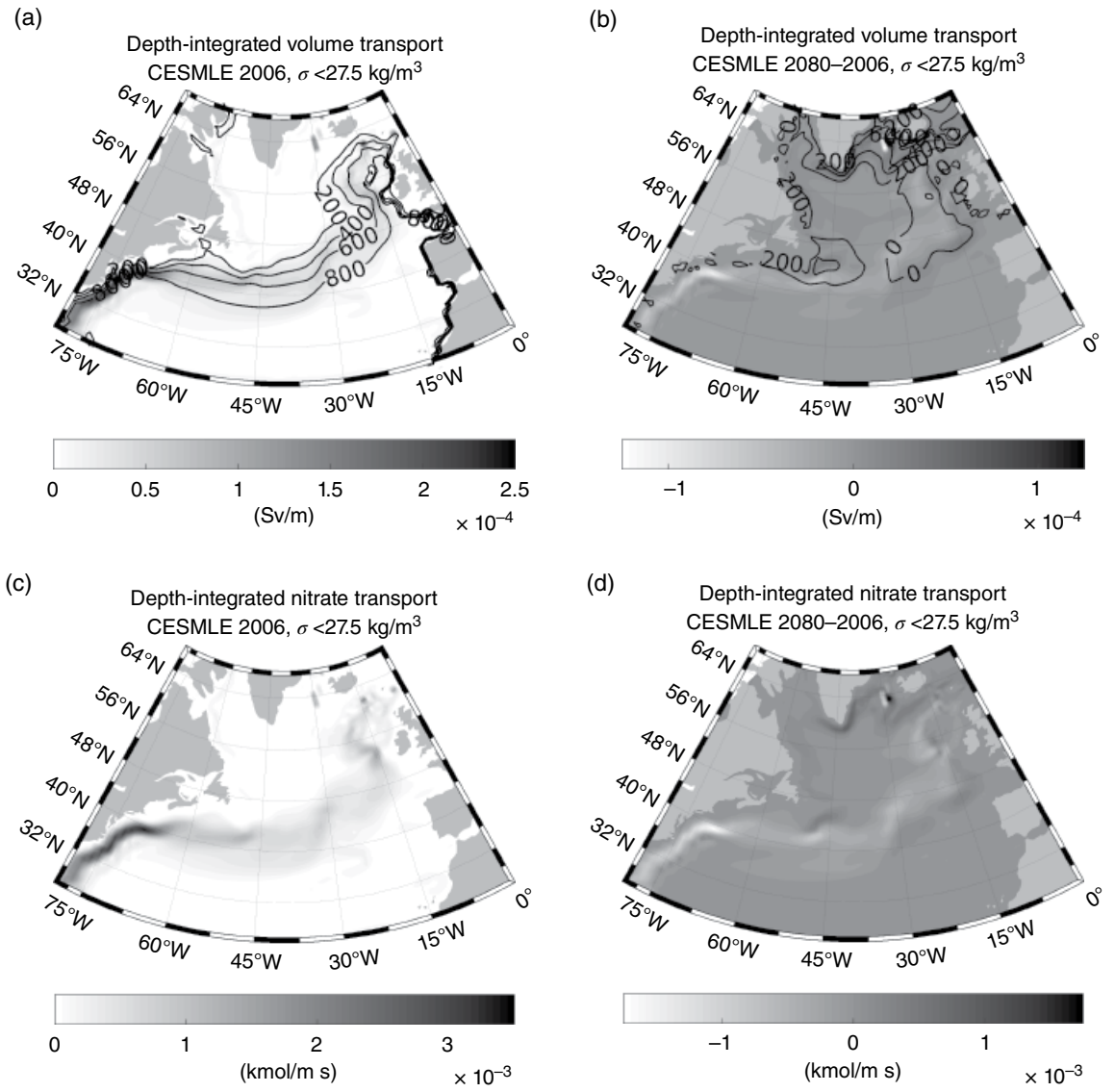

Figure 4.8 The depth-integrated, annual-and-ensemble-mean magnitude of the advective volume flux (a) and nitrate flux (c) as in Figure 4.6, but summed over an isopycnal layer $\sigma_\theta < 27.5$ and not integrated zonally across the basin. Differences between 2080 and 2006 are shown in (b), and (d). Contours in (a) show the depth of the $\sigma_\theta = 27.5$ kg/m^3 isopycnal in meters; the change in the depth of $\sigma_\theta = 27.5$ kg/m^3 between 2006 and 2080 is shown in (b). Positive numbers mean the isopycnal is deeper in 2080 than 2006.

Here, $NO3_{PYC}$ is the nitrate concentration in the first grid cell below the depth of the boundary layer and $NO3_{BL}$ is the average nitrate concentration above the depth of the boundary layer. The depth of the biologically active layer, above which phytoplankton growth can occur, is taken to be a constant $H_{BIO} = 100$ m (Figure 4.11). The coefficient Λ is an indicator function that restricts the calculation to particular locations or times. In particular, $\Lambda = 1$ when $\partial H_{BLT}/\partial t > 0$, and $\Lambda = 0$ when $\partial H_{BLT}/\partial t \leq 0$. In addition, $\Lambda = 0$ when $H_{BLT} < H_{BIO}$, and $\Lambda = 1$ when $H_{BLT} > H_{BIO}$. Finally, two different definitions are considered: one in which $\Lambda = 1$ only in the grid cells where the minimum March surface density $\sigma_\theta > 27.5$ kg/m^3, and hence at least some fraction of the annually entrained water is sourced from waters with $\sigma_\theta > 27.5$ kg/m^3; and a second in which $\Lambda = 1$ only where and when the surface density $\sigma_\theta > 27.5$ kg/m^3, and hence all of the entrained water is sourced from waters with $\sigma_\theta > 27.5$ kg/m^3. The two definitions can be viewed as conservative (high) and best estimates of the net flux of nitrate to the top 100 m that is sourced from water denser than 27.5 kg/m^3 in the subpolar gyre.

Qualitatively, the two definitions of the entrainment nitrate flux are similar; both decline significantly between

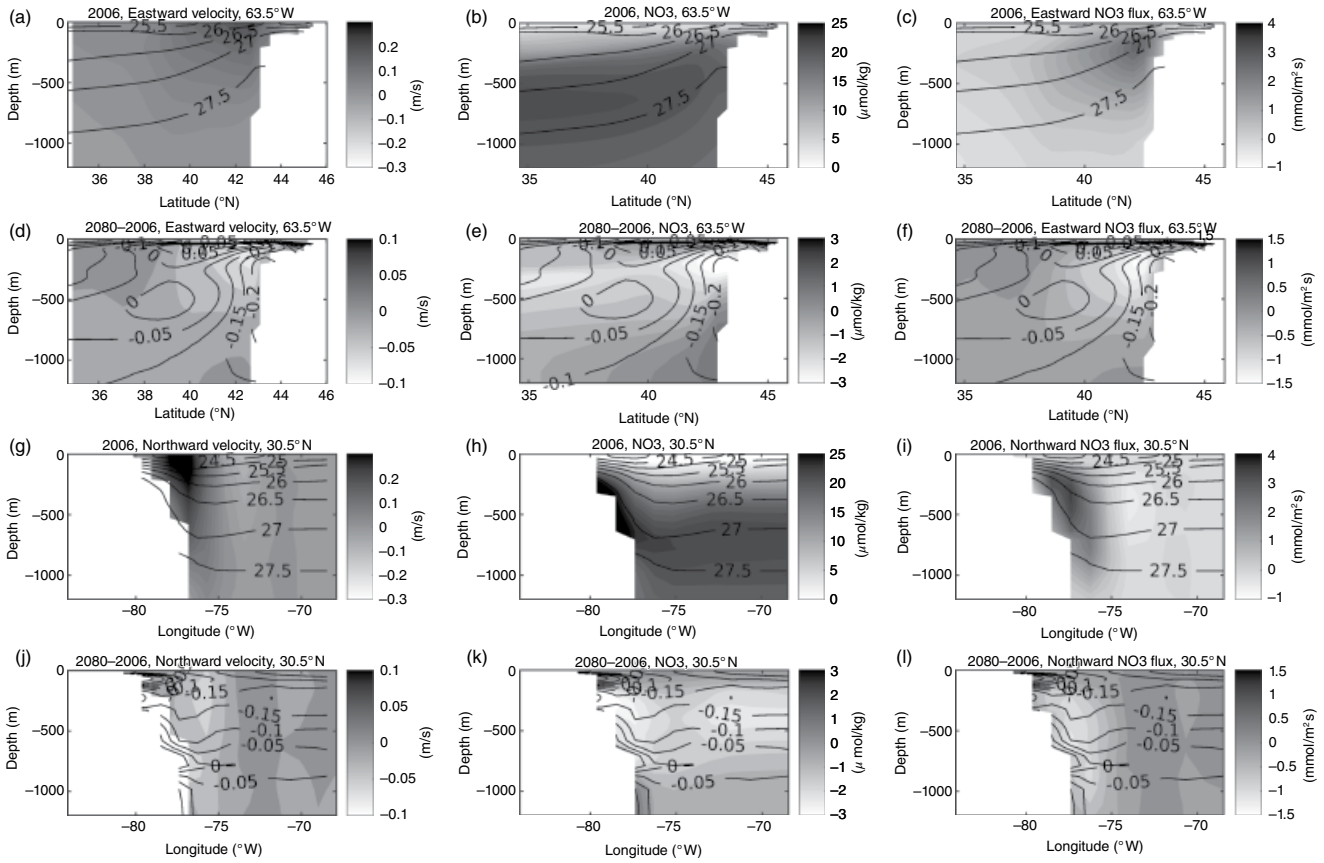

Figure 4.9 Ensemble and annual average velocity (left panels), nitrate concentration (middle panels), and nitrate flux (right panels) in two sections across the Gulf Stream in CESM1. Data from the year 2006 are shown in (a)–(c) and (g)–(i), whereas differences between 2006 and 2080 are shown in (d)–(f) and (j)–(l). Potential density contours are overlaid in black. Comparisons can be made to observations in Figure 4.2.

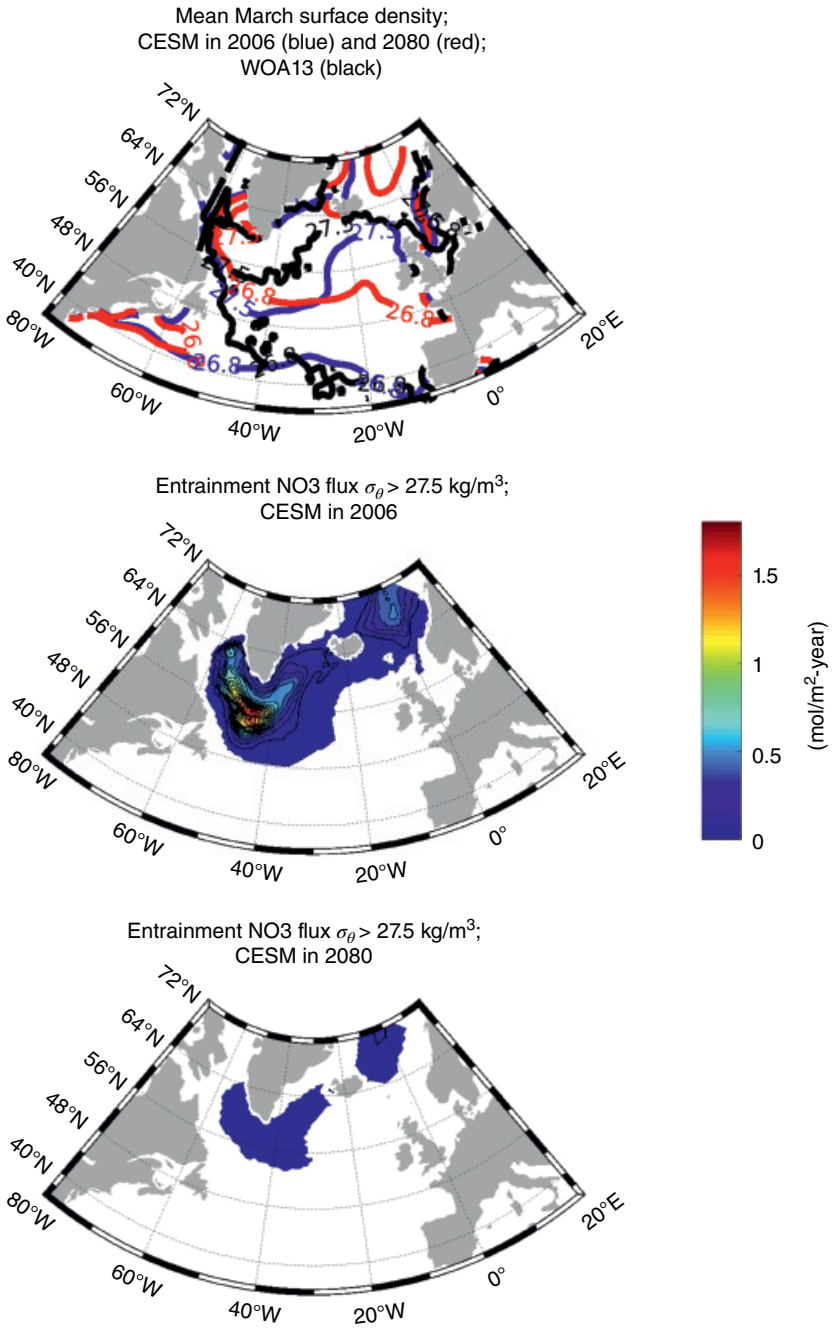

Figure 4.10 (top) The mean surface potential density in March from the ensemble of CESM1 runs during 2006 (blue) and 2080 (red). The World Ocean Atlas (WOA13) data (Boyer et al., 2013) are contoured in black for reference. The ensemble and annual mean entrainment flux of nitrate, where $\sigma_\theta > 27.5$ kg/m^3, in the CESM1 runs during 2006 (middle) and 2080 (bottom). (*See electronic version for color representation of this figure.*)

2006 and 2080 in CESM, and both are significantly smaller than the zonally-integrated advective flux above $\sigma_\theta = 27.5$ kg/m^3 at 48° N. A comparison of these two ensemble-mean and area-integrated measures of the entrainment flux shows that the first (about 75 kmol/s in 2006 and 15 kmol/s in 2080) is significantly larger than the second (about 36 kmol/s in 2006 and 1.5 kmol/s in 2080). However, both measures are significantly smaller than the zonally-integrated northward advective flux of nitrate at 48° N (about 308 kmol/s in 2006 and 177 kmol/s in 2080). In addition, the decline in the two measures of the entrainment flux between 2006 and 2080 (about 60 kmol/s and 34 kmol/s, respectively) are significantly smaller than the decline in the zonally-integrated northward advective

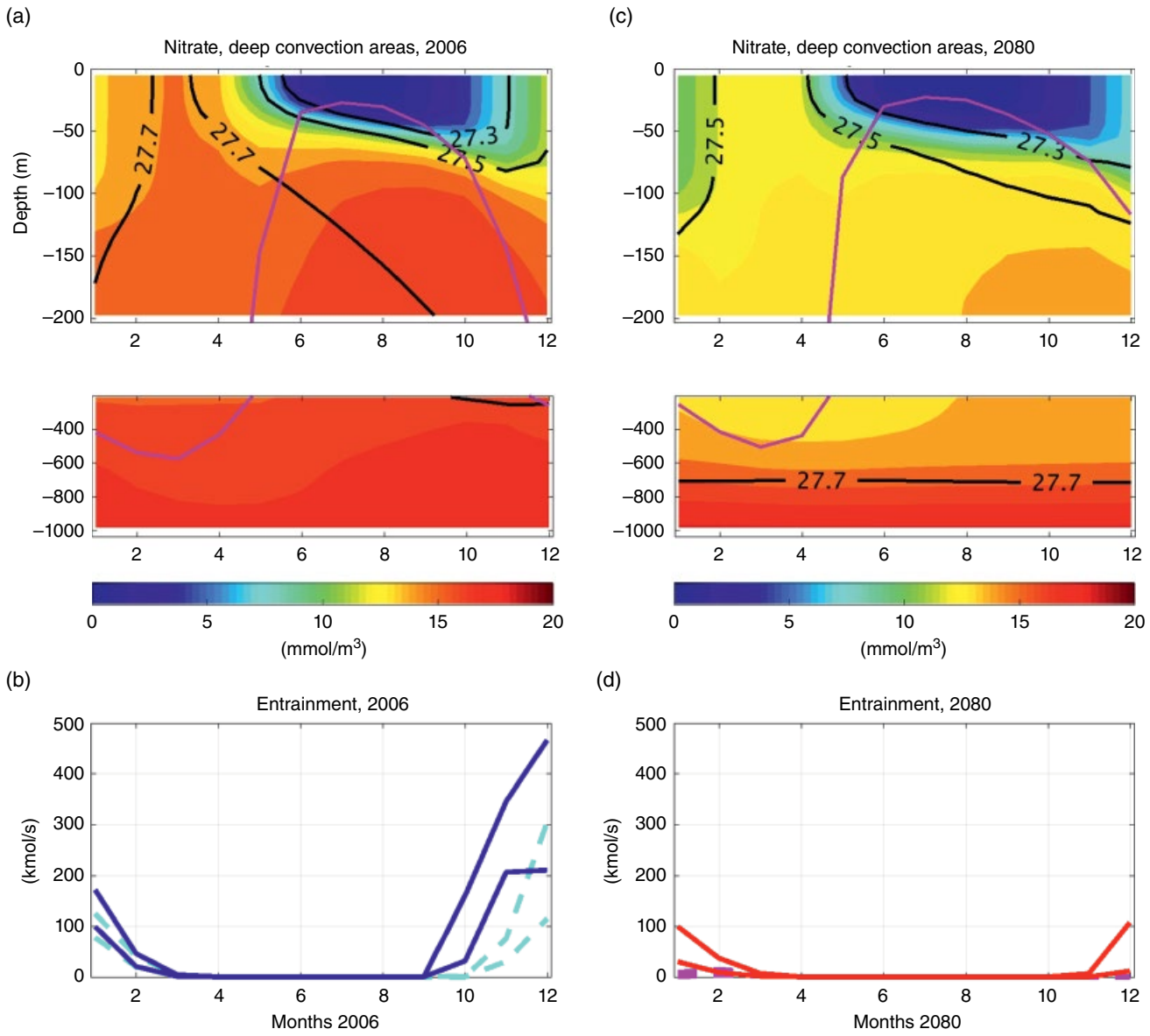

Figure 4.11 (top) Ensemble and area averaged seasonal cycle of nitrate (color), potential density (black), and boundary layer thickness (magenta) during 2006 (a) and 2080 (b) in CESM1, where the area average is over the region of the subpolar North Atlantic where the surface potential density $\sigma_\theta > 27.5$ kg/m^3 in March (see Figure 4.10). (bottom) The ensemble average entrainment nitrate flux integrated over the area where the surface potential density $\sigma_\theta > 27.5$ kg/m^3 in March (solid lines) and the area where the surface potential density $\sigma_\theta > 27.5$ kg/m^3 at the time when the entrainment occurs (dashed lines) during 2006 (b) and 2080 (d) in CESM1. (*See electronic version for color representation of this figure.*)

nitrate flux between 2006 and 2080 at 48° N (about 131 kmol/s). Figures 4.11b and 4.11d show area-integrated mean seasonal cycles of the two measures of nitrate entrainment in 2006 and 2080, and Table 4.2 reports the interquartile range for annual mean entrainment fluxes across ensemble members. Although the nitrate concentration is somewhat reduced in the area where $\sigma_\theta > 27.5$ kg/m^3 in 2080 during March (Figure 4.11), the relatively modest changes between 2006 and 2080 in the mean seasonal cycle of the boundary layer depth, density, and nitrate profiles suggests that the ~75% reduction in the annual average entrainment flux (by the March surface density definition) between 2006 and 2080 can be inferred to a good approximation from the nearly proportional 75% reduction in area where surface mixing reaches waters where $\sigma_\theta > 27.5$ kg/m^3 (see Table 4.2 and Figure 4.10).

As expected, the significant reductions in both the advective and entrainment fluxes of nitrate to isopycnals $\sigma_\theta < 27.5\,kg/m^3$ in the subpolar North Atlantic occur together with significant reductions in export production in the subpolar gyre between 2006 and 2080. The ensemble and annual average sinking flux of particulate organic nitrogen north of 48° N declines by 27% from 121 kmol/s to 88 kmol/s at 100 m depth and by 54% from 80 kmol/s to 37 kmol/s at $\sigma_\theta = 27.5\,kg/m^3$. The decline in the export flux across $\sigma_\theta = 27.5\,kg/m^3$ from 2006 to 2080 (43 kmol/s) is larger in magnitude than the corresponding reduction in the entrainment flux across $\sigma_\theta = 27.5\,kg/m^3$ (34 kmol/s). Hence, the reduction in the entrainment flux associated with winter mixing cannot possibly explain the entire reduction in export. In addition, Figure 4.12 shows that the areas where export flux across $\sigma_\theta = 27.5\,kg/m^3$ is strongest and the magnitude of the reduction in export from 2006 to 2080 is greatest are not collocated with the areas where the entrainment flux across $\sigma_\theta = 27.5\,kg/m^3$ is strongest and the reduction in entrainment from 2006 to 2080 is greatest (Figure 4.10); this supports the hypothesis that the ocean circulation plays an important role in driving export and its declines from 2006 to 2080 in the RCP8.5 scenario. Based on the relative magnitudes, it is possible to conjecture that about 20% of the reduction in export is explained by reduced winter mixing and entrainment, whereas 80% is explained by reductions in the northward advective flux. However, future work is required to assess the validity of this conjecture in more detail.

Taken together, these results suggest that the forced change in net northward volume and nitrate transport integrated across the North Atlantic basin, which manifests in a significantly reduced Gulf Stream transport in the subtropics, is of first order significance for the upper ocean nitrate budget of the North Atlantic subpolar gyre and an important mechanism driving forced declines in export production in the North Atlantic during the 21st century. But how uncertain are these model projections?

4.3.3. Discussion of Model Uncertainties

Estimates of model uncertainty can be obtained by comparing CESM1 with other Earth system models and

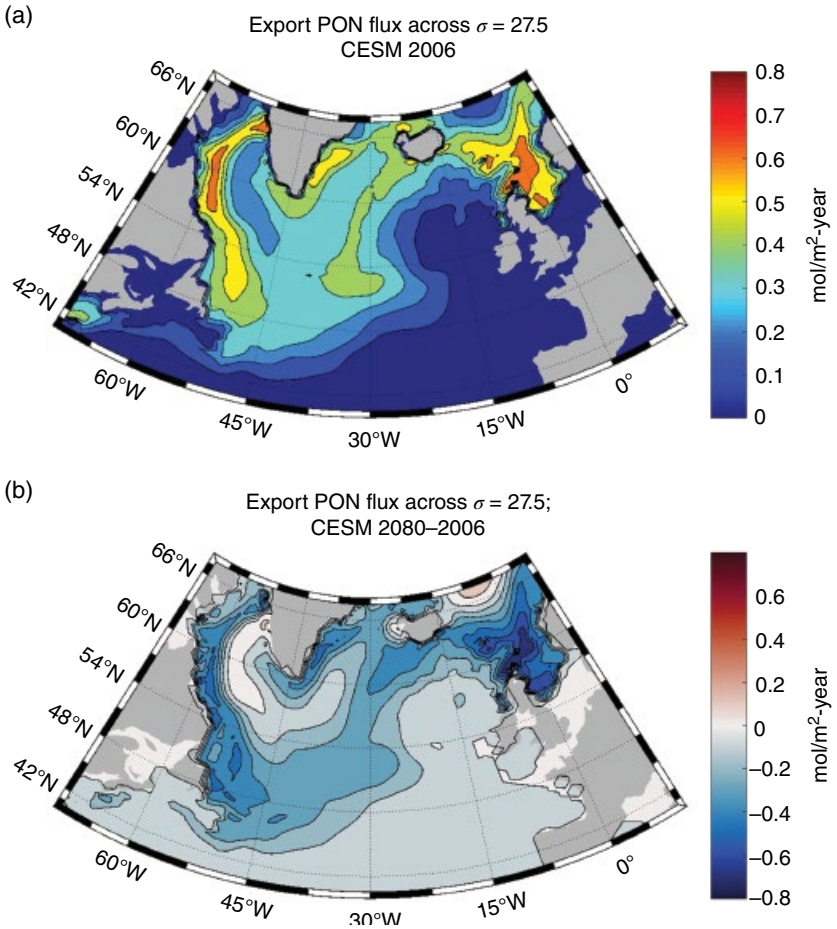

Figure 4.12 The ensemble mean export flux of particulate organic nitrogen across $\sigma_\theta = 27.5\,kg/m^3$ in CESM1 during 2006 (a) and the difference 2080-2006 (b). (*See electronic version for color representation of this figure.*)

observations. Although the qualitative result that the AMOC and associated northward nitrate transport reduce in the 21st century is expected to be robust across Earth system models, the magnitude of the reduction is expected to be model dependent. Because the volume and nitrate transport are highly correlated in CESM1, the range of the changes in nitrate transport between models can be estimated to approximately equal the 15–60% range of reductions in the AMOC volume transport during the 21st century in CMIP5 models (Cheng et al., 2013).

There may be additional uncertainty associated with the model projections that is not captured by the range of CMIP5 models. To assess these uncertainties, CESM1 has been compared with observations. A comprehensive assessment of the mean state and variability of the AMOC in CESM1 and other Earth system models in hind-casts with the CORE-2 inter-annually varying atmospheric conditions has been conducted (Danabasoglu et al., 2014, 2016). The overall conclusion is that most models are suitable for studies of the North Atlantic. To briefly summarize, CESM1 has a relatively strong AMOC compared to other models, and the maximum transport (about 25 Sv; Figure 4.6) is elevated by about 40% compared to the approximately 18 Sv maximum transport in the observations-based inverse model of Lumpkin and Speer (2007). But, the simulated AMOC in CESM1 is much closer to the inverse model away from the region of maximum transport at about 40° N. Consistent with a stronger AMOC, deep convective winter mixed layers are deeper and more extensive and surface density is greater in the Labrador and Norwegian seas compared to the World Ocean Atlas (Figure 4.10). The forced version of CESM1 also produces a relatively realistic vertical profile of AMOC transport at 26.5° N compared to observations between the years 2004 and 2007, and the meridional heat transport is consistent with several observational estimates near the latitude of maximum poleward heat transport (20–25°N) (Danabasoglu et al., 2014). However, the representation of the AMOC in the coupled version of CESM1 used here differs somewhat from the AMOC in CESM1 in the hindcast configuration forced by a prescribed atmospheric state used by Danabasoglu et al. (2014). For example, Kim et al. (2018) show that a forced hindcast produces significantly stronger and more realistic multidecadal AMOC variability than the coupled version of CESM1. However, it is not clear how this divergence between the simulations would impact the anthropogenically forced response of the coupled model during RCP8.5 21st century simulations, since Kim et al. (2018) conjecture that the deficiency in variability is attributable to low multidecadal variability in North Atlantic Oscillation, which may not directly influence the forced response to anthropogenic emissions.

In all versions of CESM1 with a free-running nominal 1° resolution ocean model, the modeled eastward Gulf Stream volume transport in the upper 2 km at 64° W is expected to be much less than the observed 70–100 Sv Gulf Stream transport but not so much smaller than the observed baroclinic transport above 1 km, which is about 47 Sv in observations and calculated by assuming a level of no motion at 1 km depth and integrating above that (Hogg, 1992). The discrepancy between the observed Gulf Stream transport and the modeled Gulf Stream transport in the nominal 1° resolution ocean model arises because there is essentially zero eddy-driven recirculation in the model Gulf Stream (which accounts for roughly 2/3 of the full-depth-integrated ~150 Sv transport at 64° W). Despite the missing recirculation and the failure of the model Gulf Stream to separate from the coast at Cape Hatteras in CESM1 (Figure 4.9), the barotropic streamfunction and barotropic vorticity budget of the North Atlantic subtropical gyre in CESM1 are expected to be qualitatively similar in configurations with a higher-resolution ocean model (Schoonover et al., 2016). For example, the modeled Gulf Stream nitrate transport above $\sigma_\theta = 27.5\,\mathrm{kg/m^3}$ in 2006 (518 kmol/s at 30.5°N and 534 kmol/s at 64°W) is larger than the observed nitrate flux through the Straits of Florida, about 300 kmol/s, and smaller than the observed flux at Cape Hatteras, about 700–800 kmol/s (Pelegrí & Csanady, 1991; Williams et al., 2011) (c.f. Figures 4.2 and 4.9). Taken together, the available evidence suggests that the CESM1 configuration used here could produce a qualitatively accurate description of current and future baroclinic nitrate transport in the Gulf Stream that is associated with the AMOC. However, the absence of mesoscale eddies and the associated barotropic recirculation gyres in the vicinity of the Gulf Stream is a key uncertainty associated with these results from CESM1, and future research is certainly needed to verify these results, particularly with higher resolution ocean models that resolve mesoscale dynamics.

4.3.4. Summary

CESM1 projects significant reductions in the northward volume and nitrate transport on upper ocean isopycnals ($\sigma_\theta < 27.5\,\mathrm{kg/m^3}$) integrated zonally across the entire North Atlantic basin during the 21st century. This reduction in the AMOC and associated nitrate transport is associated with significant reductions in the Gulf Stream volume and nitrate transport. In addition, the forced reduction in the advective nitrate flux to the mid-to-high latitudes in the North Atlantic occurs in conjunction with a significant reduction in the export flux of particulate organic nitrogen to the deep ocean. The projected reduction in the area and depth of North

Atlantic deep convection over the 21st century also reduces the total nitrate flux across $\sigma_\theta = 27.5\,kg/m^3$ to the upper ocean and the export of particulate organic nitrogen. However, scaling arguments and CESM1 results suggest that the direct effect of reductions in the vertical nitrate flux due to reductions in the area of deep convection is only about one-quarter as important for the forced change in total nitrate flux to the upper ocean in the subpolar North Atlantic compared to the reduction in the northward isopycnal advective nitrate flux due to the slowing of the AMOC during the 21st century.

Comparable forced reductions in the advective flux of other macronutrients to the upper ocean of the mid-to-high latitude North Atlantic can be expected in these CESM1 simulations of the RCP8.5 scenario because the reductions in the nitrate flux are so strongly correlated with reductions in volume transport, but an explicit accounting of the change in the advective flux of other nutrients in these simulations is left for future work. More generally, future work should systematically quantify how changes in North Atlantic atmosphere–ocean and ice–ocean buoyancy fluxes affect the relative magnitude of the horizontal advective nutrient and vertical convective nutrient supply pathways in the mid-to-high latitude North Atlantic, which depend on the strength of the coupling between air–sea buoyancy fluxes, deep convection, the AMOC, and freshwater fluxes from the Arctic. In addition, future work is needed to more precisely identify where, when, and to what degree reductions in the net advective and convective nutrient fluxes to upper ocean isopycnals in the mid-to-high latitude North Atlantic drive the forced changes in primary and export production, plankton biomass, and marine ecosystem dynamics. Finally, future work should explore the sensitivity of these results to ocean model resolution and, in, particular explore the sensitivity of the results to mesoscale dynamics.

4.4. HOW SMALL-SCALE PROCESSES MODIFY AMOC AND THE ASSOCIATED GULF STREAM NUTRIENT TRANSPORT

Although the CESM simulations suggest that the zonally-integrated meridional flux of macronutrients will decline significantly over the 21st century in the North Atlantic, the precise magnitude of the decline and the spatiotemporal details of the forced response remain somewhat uncertain. For example, the model results show that the forced response in the zonally-integrated nitrate transport in the subtropics is primarily associated with a reduction in the Gulf Stream volume transport (more so than an increase in the recirculating southward nitrate flux on upper ocean isopycnals in other parts of the basin or a reduction in nitrate concentrations in the Gulf Stream). Hence, an important question about these future projections is to what degree small-scale dynamics in the Gulf Stream and elsewhere impact the zonally-integrated meridional nurtient transport, since these small-scale processes are parameterized in Earth system models. In addition, the AMOC is known to be sensitive to the details of parameterizations of both turbulent diapycnal and isopycnal fluxes (Jayne, 2009; Marshall et al., 2017) as well as to ocean model resolution (Winton et al., 2014). Yet, separated western boundary currents in general, like the separated Gulf Stream in particular, are thought to be areas where horizontal isopycnal advection by the mean current is a dominant term in the upper ocean nutrient budget compared to vertical or isopycnal mixing or isopycnal upwelling in mesoscale and submesoscale structures on interannual and longer timescales (Olson, 2001; Letscher et al., 2016). It may be noted that the advective eddy flux term or vertical diffusive flux term contribute significantly to the supply of nutrient to the surface layer of the ocean in model diagnositc output if the depth level of interest is sufficiently shallow (e.g., 100 m), and the relative contribution may depend on model resolution. However, these "last mile" transports are essentially set by the upstream advective flux from the general circulation on interannual timescales. Thinking of this "last mile" transport as a nutrient source to the upper ocean independent of the large scale circulation can lead to confusion and apparent inconsistencies, for example the difference between the results of Oschlies (2002a) and McGillicuddy et al. (2003), in which the parameterized deep nutrient supply (representing the effect of the large scale circulation) plays a crucial role in controlling the influence on mesoscale-eddy-driven vertical nutrient fluxes and primary productivity in the subtropical North Atlantic. The conceptual model of the time-averaged nutrient budget, where advective isopycnal flux convergence is associated with induction of nutrient into the mixed layer and biological consumption, is shown in Figure 4.5. The impacts of small-scale processes may be largely indirect/remote and, hence, difficult to assess quantitatively without conducting process studies.

Despite significant uncertainty about remote impacts of small-scale processes, this section attempts to obtain estimates for the magnitudes of the contributions of various small-scale ocean processes to the nutrient budget in the Gulf Stream, all of which are parameterized in the CESM1 simulations presented here and/or poorly constrained by global observing systems and, therefore, are a potential source of uncertainty in the CESM1 projections and the conceptual model of the Gulf Stream nutrient stream. Available observations and process studies provide some guidance about plausible ranges for the effect of various small-scale processes on Gulf Stream nutrient transport. The discussion is divided into three topics:

(i) interior diapycnal mixing in the pycnocline, (ii) boundary layer processes, and (iii) mesoscale and jet-scale processes. The discussion of these processes is necessarily incomplete but the aim is to briefly assess the potential uncertainty associated with each of these processes for the Gulf Stream nutrient transport using scaling and published results in order to identify areas most in need of future research, rather than to provide a comprehensive review of the dynamics of the various processes.

4.4.1. Diapycnal Mixing in the Pycnocline

Pelegrí and Csanady (1991) were the first to lay out a coherent description of the Gulf Stream nutrient stream. In this and later work (Pelegrí & Csanady, 1994; Pelegrí et al., 1996, 2006), diapycnal mixing is suggested to be an important mechanism for transporting deep nutrients to upper ocean isopycnals in the Gulf Stream. In addition, Jenkins and Doney (2004) proposed that enhanced diapycnal mixing in the Gulf Stream could be an explanation for the discrepancy between directly measured diapycnal nutrient fluxes in the North Atlantic subtropical gyre and much larger estimates of diapycnal nutrient fluxes based on the indirect flux gauge technique.

However, no direct measurements of turbulent dissipation rates or diapycnal mixing via tracer release experiments support the hypothesis that mixing is elevated by more than one order of magnitude on average in the Gulf Stream upper pycnocline and away from boundary layers (relative to the canonical open ocean pycnocline value of 10^{-5} m^2/s). Instead, measurements of shear and temperature microstructure in the Gulf Stream (Oakey & Elliott, 1977; Gregg & Sanford, 1980; Gargett & Osborn, 1981; Winkel et al., 2002; Inoue et al., 2010a; Whitt, 2015; Lozovatsky et al., 2017), including observations during intense late-winter atmospheric forcing (Inoue et al., 2010a; Whitt, 2015), suggest that the average diapycnal diffusivity is of order 10^{-5} or 10^{-4} m^2/s. In particular, the average interior diapycnal diffusivity may be elevated by about an order of magnitude to about 10^{-4} m^2/s in the Gulf Stream pycnocline compared to regions with less energetic mesoscale flows, such as the middle of the subtropical gyre, but the data do not support a diapycnal diffusivity that is elevated by two orders of magnitude on average in the Gulf Stream pycnocline. Possible causes of enhanced turbulence and mixing in the Gulf Stream pycnocline include enhanced energy flux into near-inertial internal waves by relatively strong winter storms or hurricanes above the Gulf Stream and wave-balanced flow interactions that trap, amplify and dissipate near-inertial waves in the upper-pycnocline of the Gulf Stream's balanced fronts and eddies (Kunze et al., 1995; Inoue et al., 2010a; Polzin & Lvov, 2011; Whitt & Thomas, 2013; Joyce et al., 2013b; Whitt, 2015; Whitt et al., 2018). Observations suggest a similar enhancement of turbulent kinetic energy may be observed in other regions with energetic mesoscale flows, like the Kuroshio, and for similar reasons (Nagai et al., 2009, 2012, 2017; Whalen et al., 2012.).

The microstructure-based estimates of diapycnal diffusivity have been shown to be accurate by comparison with tracer releases elsewhere in the ocean (Ledwell et al., 1993), except in circumstances where intense mixing in boundary layers can facilitate diapycnal exchange (Watson et al., 2013; Mashayek et al., 2017). In addition, rather more extensive fine-scale measurements of density stratification and/or vertical shear of horizontal velocity on length scales between tens and hundreds of meters also suggest a diapynal diffusivity of order 10^{-4} m^2/s in the Gulf Stream pycnocline (Whalen et al., 2012), and these parameterizations have been shown to accurately represent microstructure estimates to within about a factor of 2 elsewhere in the ocean (Whalen et al., 2015).

Assuming a Gulf Stream area of about 1 million km^2, a diapycnal diffusivity of 10^{-4} m^2/s, and a vertical nitrate gradient of 10^{-4} mol/m^4 yields a diapycnal flux of about 10 kmol/s over the entire Gulf Stream, from the Straits of Florida to the Grand Banks, which is comparable in magnitude to the 20 kmol/s diapycnal flux obtained in the introduction by integrating over the entire area of the North Atlantic and assuming a diapycnal diffusivity of 10^{-5} m^2/s. However, this scaling suggests that the diapycnal nutrient flux in the upper pycnocline of the Gulf Stream is at least an order of magnitude smaller than the isopycnal advective nitrate fluxes passing into and out of the Gulf Stream region in the upper ocean. On the other hand, if for some reason the diapycnal diffusivity were 10^{-3} m^2/s (e.g., in a model with spurious numerical diffusion), then the diapycnal flux would be a major term in the overall nutrient budget of the upper ocean ($\sigma_\theta < 27.5$ kg/m^3) in the Gulf Stream (and the whole Atlantic basin). But an interior diapycnal diffusivity of 10^{-3} m^2/s is implausible, because it would imply that a large fraction of the upwelling of North Atlantic deep water and the closure of the AMOC occurs in the vicinity of the Gulf Stream, which is inconsistent with the inverse model of Lumpkin and Speer (2007) that shows North Atlantic deep water is transported to lighter isopycnals primarily in the Southern Ocean.

Although the local diapycnal nutrient flux in the Gulf Stream is certainly a small contributor to the Gulf Stream nutrient budget, the indirect effects of diapycnal mixing on the Gulf Stream transport and the nutrient budget can be significant. For example, process simulations with a predecessor to CESM with imposed atmospheric conditions show that a tenfold increase in the diapycnal diffusivity from 10^{-5} m^2/s to 10^{-4} m^2/s can double the volume transport of the AMOC, a significant part of which passes through the Gulf Stream, in a 3° resolution ocean

configuration (Jayne, 2009). However, the uncertainty associated with the diapycnal diffusivity is really more like 20% or less in Earth system models with a 1° resolution ocean (like the model used here) (Eden et al., 2014; Melet et al., 2016), because the basin-mean diapycnal diffusivity is not realistically 10^{-4} m^2/s in the pycnocline and the effects of changes in the diapycnal diffusivity are expected to be reduced in a model with a 1° resolution ocean compared to a model with a 3° resolution ocean (Jayne, 2009). However, future work should continue to assess the indirect impacts of horizontal spatial variations in diapycnal diffusivity in the pycnocline (e.g., as observed by Whalen et al., 2012) on the AMOC and Gulf Stream transport in Earth system models, including enhanced diapycnal diffusivity in the pycnocline of the Gulf Stream. In addition, future work should explore how changes in the diapycnal diffusivity in the pycnocline impact the forced response of the AMOC and the AMOC-associated part of the Gulf Stream transport to various emissions scenarios. In general, the forced response of the AMOC to anthropogenic emissions is strongly correlated to the control state of the AMOC in Earth system models (Winton et al., 2014). But, how does this relationship hold up in process studies when the differences in the control state are caused by differences in the diapycnal diffusivity in the pycnocline?

4.4.2. Boundary Layer Processes

The AMOC nutrient transport, and thereby the part of the Gulf Stream transport associated with AMOC, can also be modified by local and remote ocean boundary layer physical processes, and uncertainties in ocean boundary layer physics may introduce significant quantitative uncertainty into model projections of the associated nutrient transport. Preliminary estimates for the remote impact of changes in the surface boundary layer mixing are relatively small. Large et al. (1997) show that a very crude upper ocean vertical mixing scheme produces a similar AMOC to the nonlocal K-profile parameterization (which is used in CESM1) (Large et al., 1994) in a nominal 3° resolution ocean model, although they show that the AMOC depends relatively strongly on the surface boundary conditions. In addition, the experiments of Fox-Kemper et al. (2011) with a nominal 1° resolution ocean model show that the parameterization of mixed layer restratification by submesoscale eddies, which is used in CESM1, reduces the mixed layer depth by hundreds of meters in large areas of the North Atlantic during winter. However, this parameterization enhances the AMOC by a modest 1–2 Sv (5–10%) and presumably enhances the Gulf Stream nutrient transport by a comparably modest amount, in a somewhat unintuitive result. These results suggest reasonably small uncertainties in the projection of the AMOC and Gulf Stream nutrient fluxes due to the remote impact of surface boundary layer physics. That said, it may be worth revisiting the remote impacts of surface boundary layer physics in higher-resolution modern Earth system models. A particular concern is that the AMOC dynamics tend to be driven primarily by diapycnal mixing in the pycnocline in very coarse-resolution ocean models, whereas the AMOC tends to be driven more by air–sea fluxes in higher-resolution models, so the AMOC may be more sensitive to surface boundary layer physics in higher-resolution ocean models.

Differences in surface boundary layer physics may also have significant local impacts on the Gulf Stream nutrient budget by changing the magnitude and timing of exchanges between the surface euphotic layer, where phytoplankton grow, and upper pycnocline isopycnals. For example, the Gulf Stream may significantly modify atmospherically-forced turbulent mixing and entrainment in the ocean surface boundary layer (Marshall et al., 2009; Joyce et al., 2009, 2013a; Inoue et al., 2010b) and may therefore modify the transport of nutrient from the upper pycnocline to the mixed layer in the vicinity of the Gulf Stream. In particular, the warm water of the Gulf Stream and its mesoscale variability can significantly modify the atmosphere above it. Hence, the Gulf Stream is a region where strongly coupled air–sea interaction occurs at the ocean mesoscale (Small et al., 2008; Kelly et al., 2010; Chelton & Xie, 2010). These mesoscale air–sea interactions create mesoscale gradients in the surface wind stress and air–sea heat fluxes that induce mesoscale modulations in ocean boundary layer turbulence, entrainment, and vertical velocities that impact nutrient budgets and phytoplankton dynamics at the surface in the Gulf Stream (Gaube & McGillicuddy, 2017). In addition, mesoscale air–sea interaction has an indirect effect on Gulf Stream transport and dynamics (Ma et al., 2016; Renault et al., 2016), which may impact the mean transport of the Gulf Stream by as much as 10%. However, it is not clear whether or not mesoscale air–sea interaction would impact the anthropogenically-forced response of the AMOC, and process studies to constrain the indirect and remote impacts of mesoscale air–sea interaction on the AMOC and its forced response should be a priority for future work.

Ocean boundary layer turbulence can also be modified by ocean mesoscale-to-submesoscale processes even in the absence of explicit air-sea coupling. For example, the warm surface water of the Gulf Stream is associated with very strong air–sea heat loss during winter that energizes boundary layer turbulence and enhances turbulent entrainment in the Gulf Stream (Inoue et al., 2010a, 2010b), and these effects are not well represented in coarse-resolution ocean models. In addition, observations

and simulations show enhanced dissipation of turbulent kinetic energy in the surface boundary layer of the Gulf Stream when the wind stress is aligned with the geostrophic shear of the frontal jet (Thomas et al., 2013, 2016) and trapped and amplified near-inertial waves in the upper pycnocline (Whitt & Thomas, 2013; Whitt et al., 2018), neither of which are represented in Earth system models. However, the interactions between turbulence and strong mesoscale and submesoscale lateral variability and their implications for biogeochemistry in the Gulf Stream remain relatively poorly understood. An important challenge for future research is to assess the aggregate local impacts of lateral mesoscale-to-submesoscale variability on boundary layer turbulence, entrainment, subduction and thereby biogeochemistry in the Gulf Stream. Significant progress has been made using idealized configurations (Lévy et al., 2012), but more work is needed to explore these questions in ocean domains with realistic bathymetry and realistic atmospheric conditions above (Kuroda et al., 2018). However, isopycnals $\sigma_\theta > 26.8\,\mathrm{kg/m^3}$ are not observed to outcrop in the vicinity of the Gulf Stream (Figure 4.10). Hence, the specific dynamics of the surface boundary layer, as discussed above, only directly impact the Gulf Stream nutrient and volume transport on shallower isopycnals that outcrop there.

On the other hand, between the Straits of Florida and Cape Hatteras, the deeper isopycnal layer $26.8 < \sigma_\theta < 27.5\,\mathrm{kg/m^3}$ intersects the continental slope at depths ranging from about 100 m to 1 km (Atkinson, 1985). Lee et al. (1991) suggest that the Gulf Stream acts as a nutrient pump, which supplies nitrate to the outer continental shelf at an average rate of about 3 kmol/s in the South Atlantic Bight, from the Straits of Florida to Cape Hatteras. However, the average diapycnal diffusivity in the bottom boundary layer is not very well known, and measured values range widely from 10^{-6} to $10^{-2}\ \mathrm{m^2/s}$ in bottom boundary layers on continental shelves and slopes, depending on the time period that is averaged and location (Houghton & Visbeck, 1998; Winkel et al., 2002; Barth et al., 2004; Hales et al., 2009; Kunze et al., 2012; Lozovatsky et al., 2017). But, interannual and large-scale average values of order $10^{-3}\ \mathrm{m^2/s}$ or greater are not supported by the available data. In addition, the vertical nitrate gradient below the mixed layer varies by over two orders of magnitude at coastal margins, which introduces an additional uncertainty. For example, in the Straits of Florida the vertical nitrate gradient below the mixed layer varies from 2×10^{-3} to $1 \times 10^{-5}\ \mathrm{mol/m^4}$ (Zhang et al., 2017).

Inverse models of the AMOC volume transport (Lumpkin & Speer, 2007) rule out a diapycnal nutrient and volume flux that is comparable to the Gulf Stream advective nutrient and volume transport through the Straits of Florida. But, diapycnal fluxes of up to perhaps 30 kmol/s and 3 Sv in the bottom boundary layer are not easily ruled out by basin-scale inverse models. However, this maximum is much larger than estimates for the diapycnal nitrate flux across $\sigma_\theta = 27.5\,\mathrm{kg/m^3}$ based on observations of diapycnal velocities and diffusivities in bottom boundary layers. In particular, the directly estimated diapycnal flux in the bottom boundary layer is 0.01–1.25 kmol/s, assuming an average diapycnal velocity ranging from 4×10^{-6} to 5×10^{-4} m/s (based on Houghton & Visbeck, 1998; Barth et al., 2004; Kunze et al., 2012), a nitrate concentration of $25\,\mathrm{mmol/m^3}$ (Atkinson, 1985) (Figure 4.2), a bottom boundary layer depth of 100 m, and a coastline length of 1000 km. It is possible that the diapycnal fluxes are actually much higher than these direct estimates (which come from other locations/depths in the ocean). However, it seems unlikely that they are responsible for the entire 3 kmol/s net flux onto the shelf estimated by Lee et al. (1991), because much of this flux can apparently be explained by isopycnal transport during events when the pycnocline shoals due to upwelling-favorable winds and an isopycnal pathway opens between high-nutrient isopycnals in the Gulf Stream and the shelf (Lee & Atkinson, 1983; McClain et al., 1984; Lee et al., 1991; Hyun & He, 2010). Although determining the diapycnal flux in the bottom boundary with more precision is important for assessing the Gulf Stream's role in modifying the nutrient budget of the continental shelf, remaining uncertainties are unlikely to be a dominant source of uncertainty in the nutrient budget of the Gulf Stream.

4.4.3. Mesoscales Dynamics

Numerous process studies have explored the influence of mesoscale dynamics on the Gulf Stream, particularly by varying ocean model resolution, bathymetry resolution, and parameterizations (Bryan et al., 2007; Chassignet & Marshall, 2008; Schoonover et al., 2016; Saba et al., 2016). In addition, a number of studies with coupled regional physical-biogeochemical models have explored how mesoscale dynamics modifies the local biogeochemistry in the North Atlantic (McGillicuddy et al., 2003; Oschlies, 2002a, 2002b). However, the implications of local Gulf Stream mesoscale and jet-scale dynamics for intergyre and global scale transports of volume and nutrients associated with AMOC are difficult to assess due to the computational challenge associated with simulating the basin-to-global scale circulation and biogeochemistry simultaneously with mesoscales and jet scales, which span 3–4 orders of magnitude in horizontal length scales and time scales (from 10 to 10,000 km and from days to centuries). Some of the existing results highlight the importance of studying these remote effects explicitly. For example, Oschlies (2002a) show that mesoscale processes locally enhance vertical nutrient fluxes and

primary production, but the long-time and large-scale remote effects of these small-scale processes compensate for and reduce their local effect in a simulation of the North Atlantic basin. This result was more recently echoed by Lévy et al. (2012), who report similar compensating local and remote effects of submesoscale processes an idealized North Atlantic model configuration. Recent efforts to run such global high-resolution simulations indicate that changes in mesoscale and jet-scale dynamics, associated only with refinements in the ocean model resolution, can influence the AMOC transport by a significant percentage in coupled Earth system models (McClean et al., 2011; Winton et al., 2014; Gent, 2017) and therefore Gulf Stream nutrient transport and the fate of Gulf Stream nutrients, although the AMOC is only a part of the Gulf Stream transport and the forced changes in the Gulf Stream and AMOC are not necessarily linked. However, the detailed mechanisms that give rise to these changes remain poorly constrained. In particular, it is not yet clear that the low resolution of the ocean systematically biases the AMOC in either the control simulations or the transient 21st century simulations, which are highly correlated across Earth system models with widely varying ocean resolutions (Winton et al., 2014; Gent, 2017). However, it is clear that changes in ocean-model resolution alone can produce changes in various measures of the AMOC sensitivity that are comparable in magnitude to the 15–60% range of variations in AMOC found in intermodel comparisons. Hence, the uncertainty associated with mesoscale and jet-scale ocean dynamics is plausibly of a comparable magnitude to the total uncertainty. Hence, quantifying the impacts of ocean mesoscales on the AMOC and Gulf Stream volume and nutrient transports in past, current, and future climates should be a top priority for future research.

4.4.4. Summary

There are significant outstanding uncertainties about the direct/local impacts of small-scale processes, including diapycnal mixing in the pycnocline, surface and bottom boundary layer dynamics, and mesoscale dynamics on local nutrient budgets in the Gulf Stream. However, the considerable research that has been done suggests that neither diapycnal mixing in the pycnocline nor boundary layer processes are associated with order-one or even 10% uncertainties in the local nutrient budget of the Gulf Stream as a whole, because their impacts are so small. On the other hand, uncertainty about mesoscale processes, including their impact on isopycnal mixing, probably introduces the greatest uncertainty into our understanding of and ability to simulate the Gulf Stream nutrient budgets in global Earth system models. Yet, the consistency between various extant observations and simulations suggest that although this uncertainty may be greater than 10%, it is significantly less than 100%. However, the remote/indirect impacts of all three small-scale processes are much less well understood. And all of these processes may introduce indirect/remote uncertainties of 10% or more to the Gulf Stream transport as well as the part of AMOC that flows through the Gulf Stream.

4.5. CONCLUSIONS AND OUTLOOK

Observations demonstrate that the Gulf Stream advects nutrients poleward at globally significant rates and is therefore a crucial component in global biogeochemical cycles and the Earth system. In addition, observations show that the Gulf Stream nutrient transport is highly correlated with Gulf Stream volume transport. Therefore, any significant changes in Gulf Stream volume transport will tend to be associated with significant changes in Gulf Stream nutrient transport with implications for biogeochemical dynamics downstream. Consistent with this inference, an ensemble of runs with the Community Earth System Model show that anthropogenically-forced declines in Gulf Stream volume transport are associated with similar declines in Gulf Stream nitrate transport in the RCP8.5 emissions scenario. In CESM, these reductions are associated with reductions in the zonally-integrated transports of AMOC. Hence, scaling suggests that the projected 35% decline in Gulf Stream nitrate flux (above $\sigma_\theta = 27.5\,\mathrm{kg/m^3}$) is a dominant driver of the projected 54% decline in the export of particulate organic matter (across $\sigma_\theta = 27.5\,\mathrm{kg/m^3}$) in the subpolar North Atlantic between 2006 and 2080. However, future work is needed to precisely quantify the relationship between changes in Gulf Stream nutrient transport, AMOC nutrient transport, and changes in North Atlantic biogeochemistry and ecosystems. In addition, the projected impacts on the nutrient fluxes are only as robust as the projected changes in the circulation. Based on the spread in the forced response of the AMOC to RCP8.5 forcing in CMIP5 models, the qualitative declines in the part of the AMOC circulation that passes through the Gulf Stream and the associated nutrient flux are robust, but the magnitude of the declines are uncertain between 15% and 60%. Qualitatively, this model uncertainty reflects uncertainty about the fundamental dynamics of AMOC (see section 4.3 of Buckley & Marshall, 2016). Further review of the literature suggests that the results of the model simulations are unlikely to be very sensitive to realistic changes in small-scale ocean mixing at boundary layers or in the interior. However, the results may be sensitive to ocean mesoscale processes and ocean model resolution due to the potentially strong indirect/remote impact of ocean model resolution on Atlantic meridional overturning.

Some objectives for future work include studies to elucidate:

• how changes in North Atlantic atmosphere–ocean and ice–ocean buoyancy fluxes affect the relative magnitude of the horizontal advective nutrient and vertical convective nutrient supply pathways in the mid-to-high latitude North Atlantic;

• where, when, and to what degree reductions in the net advective and convective nutrient fluxes to upper ocean isopycnals in the mid-to-high latitude North Atlantic drive the forced changes in primary and export production, plankton biomass, and marine ecosystem dynamics;

• the sensitivity of the forced changes in nutrient circulation, nutrient entrainment and export production in the North Atlantic during the 21st century of the RCP8.5 scenario in CESM1 to ocean model resolution in general and explicit mesoscale dynamics in particular;

• how mesoscale air–sea interaction impacts the anthropogenically-forced response of the Gulf Stream and Atlantic meridional overturning;

• the local impacts of lateral mesoscale-to-submesoscale ocean variability in the ocean mixed layer on entrainment, subduction and thereby biogeochemistry in the Gulf Stream and the North Atlantic Current;

• how the diapycnal diffusivity in the pycnocline impacts the forced response of the AMOC to various emissions scenarios in ocean models.

Finally, the results highlight the continuing significance of sustained observations of Gulf Stream and North Atlantic Current nutrients and volume transport, since these measures may be important harbingers of regional to global biogeochemical change.

ACKNOWLEDGMENTS

I am grateful to acknowledge constructive comments on a previous draft from Matthew Long and two anonymous reviewers and useful discussions with Elizabeth Maroon, Gokhan Danabasoglu, Jessica Luo, Stephen Yeager, Justin Small, Keith Lindsay, Who Kim, and Frank Bryan.

The National Center for Atmospheric Research is supported by the National Science Foundation. I was supported by NSF awards OPP-1501193 and OCE-1658541.

Finally, this work would not have been possible without the hard work of many to obtain and process the observations and run and process the model simulations presented here. All of the data and model output used in this paper is archived online and documented, including the world ocean database (https://www.nodc.noaa.gov/OC5/WOD13/), the biogeochemical argo float data (http://biogeochemical-argo.org), and CESM Large Ensemble output (https://www.earthsystemgrid.org/dataset/ucar.cgd.ccsm4.CESM_CAM5_BGC_LE.html).

REFERENCES

Atkinson, L. (1985), Hydrography and nutrients of the southeastern us continental shelf. In L. P. Atkinson, D. W. Menzel, & K. A. Bush (Eds.), *Oceanography of the southeastern US continental shelf* (pp. 77–92), American Geophysical Union, Washington, DC.

Barth, J. A., D. Hebert, A. C. Dale, & D. S. Ullman (2004), Direct observations of along-isopycnal upwelling and diapycnal velocity at a shelfbreak front, *Journal of Physical Oceanography*, *34*(3), 543–565.

Barton, A. D., M. S. Lozier, & R. G. Williams (2015), Physical controls of variability in North Atlantic phytoplankton communities, *Limnology and Oceanography*, *60*(1), 181–197.

Beaugrand, G., P. C. Reid, F. Ibañez, J. A. Lindley, & M. Edwards (2002), Reorganization of North Atlantic marine copepod biodiversity and climate, *Science*, *296*(5573), 1692–1694.

Behrenfeld, M. J., & E. S. Boss (2014), Resurrecting the ecological underpinnings of ocean plankton blooms, *Annual Review of Marine Science*, *6*, 167–194.

Bopp, L., L. Resplandy, J. C. Orr, S. C. Doney, J. P. Dunne, M. Gehlen, et al. (2013), Multiple stressors of ocean ecosystems in the 21st century: projections with CMIP5 models, *Biogeosciences*, *10*, 6225–6245.

Bower, A. S., & T. H. Rossby (1989), Evidence of cross-frontal exchange process in the Gulf Stream based on RAFOS float data, *Journal of Physical Oceanography*, *19*, 1177–1190.

Bower, A. S., H. T. Rossby, & J. L. Lillibridge (1985), The Gulf Stream: Barrier or Blender? *Journal of Physical Oceanography*, *15*(1), 24–32.

Boyer, T. P., J. I. Antonov, O. K. Baranova, C. Coleman, H. E. Garcia, A. Grodsky, et al. (2013), *World Ocean Database 2013*, NOAA Atlas NESDIS 72.

Brambilla, E., & L. D. Talley (2006), Surface drifter exchange between the North Atlantic subtropical and subpolar gyres., *Journal of Geophysical Research*, *111*, C07,026.

Bronselaer, B., L. Zanna, D. R. Munday, & J. Lowe (2016), The influence of southern ocean winds on the north atlantic carbon sink, *Global Biogeochemical Cycles*, *30* (6), 844–858.

Bryan, F. O., M. W. Hecht, & R. D. Smith (2007), Resolution convergence and sensitivity studies with North Atlantic circulation models. *Part i: The western boundary current system, Ocean Modelling*, *16*(3–4), 141–159.

Buckley, M. W., & J. Marshall (2016), Observations, inferences, and mechanisms of the atlantic meridional overturning circulation: A review, *Reviews of Geophysics*, *54*(1), 5–63.

Buesseler, K. O., & P. W. Boyd (2009), Shedding light on processes that control particle export and flux attenuation in the twilight zone of the open ocean, *Limnology and Oceanography*, *54*(4), 1210–1232.

Burkholder, K. C., & M. S. Lozier (2011), Subtropical to subpolar pathways in the north atlantic: Deductions from Lagrangian trajectories, *Journal of Geophysical Research: Oceans*, *116*, C07017, doi: 10.1029/2010JC006697.

Burkholder, K. C., & M. S. Lozier (2014), Tracing the pathways of the upper limb of the North Atlantic meridional overturning circulation, *Geophysical Research Letters*, *41*(12), 4254–4260.

Carr, M.-E., & H. T. Rossby (2001), Pathways of The North Atlantic current from surface drifters and subsurface floats, *Journal of Geophysical Research: Oceans*, *106*(C3), 4405–4419.

Chassignet, E. P., & D. P. Marshall (2008), Gulf Stream separation in numerical ocean models. In M. W. Hecht, & H. Hasumi (Eds.), *Ocean modeling in an eddying regime* (pp. 39–61), American Geophysical Union, Washington, DC.

Chelton, D. B., & S.-P. Xie (2010), Coupled ocean-atmosphere interaction at oceanic mesoscales, *Oceanography*, *23*(4), 52–69.

Cheng, W., J. C. Chiang, & D. Zhang (2013), Atlantic meridional overturning circulation (AMOC) in CMIP5 models: RCP and historical simulations, *Journal of Climate*, *26*(18), 7187–7197.

Danabasoglu, G., S. G.Yeager, D. Bailey, E. Behrens, M. Bentsen, D. Bi, et al. (2014), North Atlantic simulations in coordinated ocean-ice reference experiments phase II (CORE-II). Part I: Mean states, *Ocean Modelling*, *73*, 76–107.

Danabasoglu, G., S. G.Yeager, D. Bailey, E. Behrens, M. Bentsen, D. Bi, et al. (2016), North Atlantic simulations in coordinated ocean-ice reference experiments phase II (CORE-II). Part II: Inter-annual to decadal variability, *Ocean Modelling*, *97*, 65–90.

Doddridge, E. W., D. P. Marshall, & A. M. Hogg (2016), Eddy cancellation of the Ekman cell in subtropical gyres, *Journal of Physical Oceanography*, *46*(10), 2995–3010, doi: 10.1175/JPO-D-16-0097.1.

Doney, S. C., M. Ruckelshaus, J. E. Duffy, J. P. Barry, F. Chan, C. A. English, et al. (2012), Climate change impacts on marine ecosystems, *Annual Review of Marine Science*, *4*, 11–37.

Dutkiewicz, S., J. R. Scott, & M. Follows (2013), Winners and losers: Ecological and biogeochemical changes in a warming ocean, *Global Biogeochemical Cycles*, *27*(2), 463–477.

Eden, C., L. Czeschel, & D. Olbers (2014), Toward energetically consistent ocean models, *Journal of Physical Oceanography*, *44*(12), 3160–3184.

Edwards, M., & A. J. Richardson (2004), Impact of climate change on marine pelagic phenology and trophic mismatch, *Nature*, *430*(7002), 881.

Fox-Kemper, B., G. Danabasoglu, R. Ferrari, S. Griffies, R. Hallberg, M. Holland, et al. (2011), Parameterization of mixed layer eddies. III: Implementation and impact in global ocean climate simulations, *Ocean Modelling*, *39* (1–2), 61–78.

Frölicher, T., F. Joos, G.-K. Plattner, M. Steinacher, and S. C. Doney (2009), Natural variability and anthropogenic trends in oceanic oxygen in a coupled carbon cycle–climate model ensemble, *Global Biogeochemical Cycles*, *23* (1).

Gargett, A., and T. Osborn (1981), Small-scale shear measurements during the fine and microstructure experiment (FAME), *Journal of Geophysical Research*, *86*, 1929–1944.

Gaube, P., and D. J. McGillicuddy (2017), The influence of Gulf Stream eddies and meanders on near-surface chlorophyll, *Deep Sea Research Part I: Oceanographic Research Papers*, *122*, 1–16.

Gent, P. R. (2017), A commentary on the Atlantic meridional overturning circulation stability in climate models, *Ocean Modelling*, *122*, 57–66.

Gent, P. R., & J. C. McWilliams (1990), Isopycnal mixing in ocean circulation models, *Journal of Physical Oceanography*, *20*(1), 150–155.

Gregg, M. C., & T. B. Sanford (1980), Signatures of mixing from the Bermuda slope, the Sargasso Sea and the Gulf Stream., *Journal of Physical Oceanography*, *10*, 105–127.

Hakkinen, S., & P. B. Rhines (2009), Shifting surface currents in the northern North Atlantic Ocean, *Journal of Geophysical Research: Oceans*, *114*(C4).

Hales, B., D. Hebert, & J. Marra (2009), Turbulent supply of nutrients to phytoplankton at the New England shelf break front, *Journal of Geophysical Research: Oceans*, *114*(C5).

Halkin, D., & T. Rossby (1985), The structure and transport of the Gulf Stream at 73 W, *Journal of Physical Oceanography*, *15*(11), 1439–1452.

Hogg, N. G. (1992), On the transport of the Gulf Stream between Cape Hatteras and the Grand Banks, *Deep Sea Research Part A. Oceanographic Research Papers*, *39*(7–8), 1231–1246.

Houghton, R. W., & M. Visbeck (11998), Upwelling and convergence in the middle Atlantic bight shelfbreak front, *Geophysical Research Letters*, *25*(15), 2765–2768.

Hyun, K. H., & R. He (2010), Coastal upwelling in the south Atlantic bight: A revisit of the 2003 cold event using long term observations and model hindcast solutions, *Journal of Marine Systems*, *83*(1–2), 1–13.

Inoue, R., M. C. Gregg, & R. R. Harcourt (2010a), Mixing rates across the Gulf Stream, Part 1: On the formation of Eighteen Degree Water, *Journal of Marine Research*, *68*, 643–671.

Inoue, R., R. Harcourt, & M. Gregg (2010b), Mixing rates across the Gulf Stream, Part 2: Implications for nonlocal parameterization of vertical fluxes in the surface boundary layers, *Journal of Marine Research*, *68*(5), 673–698.

Jayne, S. R. (2009), The impact of abyssal mixing parameterizations in an ocean general circulation model, *Journal of Physical Oceanography*, *39* (7), 1756–1775.

Jenkins, W. J., & S. C. Doney (2004), The subtropical nutrient spiral, *Global Biogeochemical Cycles*, *17*(4), 1110, doi: 10.1029/2003GB002085.

Johns, E., D. R. Watts, & H. T. Rossby (1989), A test of geostrophy in the Gulf Stream, *Journal of Geophysical Research: Oceans*, *94*(C3), 3211–3222.

Johns, W., T. Shay, J. Bane, & D. Watts (1995), Gulf stream structure, transport, and recirculation near 68 W, *Journal of Geophysical Research: Oceans*, *100* (C1), 817–838.

Johnson, K. S.., L. J. Coletti, H. W. Jannasch, C. M. Sakamoto, D. D. Swift, & S. C. Riser (2013), Long-term nitrate measurements in the ocean using the in situ ultraviolet spectrophotometer: sensor integration into the apex profiling float, *Journal of Atmospheric and Oceanic Technology*, *30* (8), 1854–11866.

Johnson, K. S., J. N. Plant, L. J. Coletti, H. W. Jannasch, C. M. Sakamoto, S. C. Riser et al. (2017), Biogeochemical sensor performance in the SOCCOM profiling float array, *Journal of Geophysical Research: Oceans*, *122*(8).

Joyce, T. M., L. N. Thomas, & F. Bahr (2009), Wintertime observations of subtropical mode water formation within the Gulf Stream, *Geophysical Research Letters*, *36*(2).

Joyce, T., L. N. Thomas, W. K. Dewar, & J. B. Girton (2013a), Eighteen degree water formation within the Gulf Stream: a new paradigm arising from CLIMODE., *Deep Sea Research II*, *91*, 1–10.

Joyce, T., J. Toole, P. Klein, & L. Thomas (2013b), A near-inertial mode observed within a Gulf Stream warm core ring., *Journal of Geophysical Research*, *118*, 1–10, doi: 10.1002/jgrc.20141.

Kay, J., C. Deser, A. Phillips, A. Mai, C. Hannay, G. Strand, et al. (2015), The community Earth system model (CESM) large ensemble project: A community resource for studying climate change in the presence of internal climate variability, *Bulletin of the American Meteorological Society*, *96*(8), 1333–1349.

Kelly, K. A., R. J. Small, R. Samelson, B. Qiu, T. M. Joyce, Y.-O. Kwon, & M. F. Cronin (2010), Western boundary currents and frontal air–sea interaction: Gulf Stream and Kuroshio Extension, *Journal of Climate*, *23*(21), 5644–5667.

Kim, W. M., S. Yeager, P. Chang, & G. Danabasoglu (2018), Low-frequency North Atlantic climate variability in the community earth system model large ensemble, *Journal of Climate*, *31*(2), 787–813.

Klocker, A., & R. Abernathey (2014), Global patterns of mesoscale eddy properties and diffusivities, *Journal of Physical Oceanography*, *44*(3), 1030–1046.

Krauss, W. (1986), The North Atlantic current, *Journal of Geophysical Research: Oceans*, *91*(C4), 5061–50744.

Krumhardt, K. M., N. S. Lovenduski, M. C. Long, & K. Lindsay (2017), Avoidable impacts of ocean warming on marine primary production: Insights from the CESM ensembles, *Global Biogeochemical Cycles*, *31*(1), 114–133.

Kunze, E. (2017), The internal-wave-driveen meridional overturning circulation, *Journal of Physical Oceanography*, *47*(11), 2673–2689.

Kunze, E., C. MacKay, E. E. McPheee-Shaw, K. Morrice, J. B. Girton, & S. R. Terker (2012), Turbulent mixing and exchange with interior waters on sloping boundaries, *Journal of Physical Oceanography*, *42*(6), 910–927.

Kunze, E., R. W. Schmidt, & J. M. Toole (1995), The energy balance in a warm core rings near-inertial critical layer, *Journal of Physical Oceanography*, *25*, 942–957.

Kuroda, H., A. Takasuka, Y. Hirota, T. Kodama, T. Ichikawa, D. Takahashi, et al. (2018), Numerical experiments based on a coupled physical–biochemical ocean model to study the Kuroshio-induced nutrient supply on the shelf-slope region off the southwestern coast of Japan, *Journal of Marine Systems*, *179*, 38–54.

Large, W. G., G. Danabasoglu, S. C. Doney, & J. C. McWilliams (1997), Sensitivity to surface forcing and boundary layer mixing in a global ocean model: Annual-mean climatology, *Journal of Physical Oceanography*, *27*(11), 2418–2447.

Large, W. G., J. C. McWilliams, & S. C. Doney (1994), Oceanic vertical mixing: A review and a model with a nonlocal boundary layer parameterization, *Reviews of Geophysics*, *32*, 363–403.

Ledwell, J. R., A. J. Watson, & C. S. Law (1993), Evidence for slow mixing across the pycnocline from an open-ocean tracer release experiment, *Nature*, *364*, 701–703.

Lee, T. N., & L. P. Atkinson (1983), Low-frequency current and temperature variability from Gulf Stream frontal eddies and atmospheric forcing along the southeast us outer continental shelf, *Journal of Geophysical Research: Oceans*, *88*(C8), 4541–44567.

Lee, T. N., J. A. Yoder, & L. P. Atkinson (1991), Gulf stream frontal eddy influence on productivity of the southeast us continental shelf, *Journal of Geophysical Research: Oceans*, *96*(C12), 22,191–22,205.

Letscher, R. T., F. Primeau, & J. K. Moore (2016), Nutrient budgets in the subtropical ocean gyres dominated by lateral transport, *Nature Geoscience*, *9*(11), ngeo2812.

Lévy, M., D. Iovino, L. Resplandy, P. Klein, G. Madec, A.-M. Tréguier, et al. (2012), Large-scale impacts of submesoscale dynamics on phytoplankton: Local and remote effects, *Ocean Modelling*, *43*, 77–93.

Lewis, M. R., W. G. Harrison, N. S. Oakey, D. Herbert, & T. Platt (1986), Vertical nitrate fluxes in the oligotrophic ocean., *Science (Washington)*, *234*(4778), 870–872.

Lindsay, K., G. B. Bonan, S. C. Doney, F. M. Hoffman, D. M. Lawrence, M. C. Long, et al. (2014), Preindustrial-control and twentieth-century carbon cycle experiments with the earth system model CESM1 (BGC), *Journal of Climate*, *27*(24), 8981–9005.

Long, M. C., C. Deutsch, & T. Ito (2016), Finding forced trends in oceanic oxygen, *Global Biogeochemical Cycles*, *30*(2), 381–397.

Long, M. C., K. Lindsay, S. Peacock, J. K. Moore, & S. C. Doney (2013), Twentieth- century oceanic carbon uptake and storage in CESM1 (BGC), *Journal of Climate*, *26*(18), 6775–6800.

Lovenduskii, N. S., G. A. McKinley, A. R. Fay, K. Lindsay, & M. C. Long (2016), Partitioning uncertainty in ocean carbon uptake projections: Internal variability, emission scenario, and model structure, *Global Biogeochemical Cycles*, *30*(9), 1276–1287.

Lozier, S. M., S. Bacon, A. S. Bower, S. A. Cunningham, M. F. de Jong, L. de Steur, et al. (2017), Overturning in the subpolar North Atlantic program: a new international ocean observing system, *Bulletin of the American Meteorological Society*, *98*(4), 737–752.

Lozovatsky, I., J. Planellla-Morato, K. Shearman, Q. Wang, & H. J. S. Fernando (2017), Vertical mixing and elements of mesoscale dynamics over North Carolina shelf and contiguous Gulf Stream waters, *Ocean Dynamics*, *67*(6), 783–798.

Lumpkin, R., & K. Speer (2007), Global ocean meridional overturning, *Journal of Physical Oceanography*, *37*(10), 2550–2562.

Ma, X., Z. Jing, P. Chang, X. Liu, R. Montuoro, R. J. Small, et al. (2016), Western boundary currents regulated by interaction between ocean eddies and the atmosphere, *Nature*, *535*(7613), 533.

Marinov, I., S. C. Doney, & I. Lima (2010), Response of ocean phytoplankton community structure to climate change over the 21st century: partitioning the effects of nutrients, temperature and light, *Biogeosciences*, *7*(12), 3941.

Marinov, I., S. C. Doney, I. D. Lima, K. Lindsay, J. K. Moore, & N. Mahowald (2013), North-south asymmetry in the modeled phytoplankton community response to climate change over the 21st century, *Global Biogeochemical Cycles*, *27*(4), 1274–1290.

Marshall, J., R. Ferrar, G. Forget, G.Maze, A. Andersson, N. R. Bates, et al. (2009), The CLIMODE field campaign: Observing the cycle of convection and restratification over the Gulf Stream, *Bulletin of the American Meteorological Society*, *90*, 1337–1350.

Marshall, J., & F. Schott (1999), Open-ocean convection: Observations, theory, and models, *Reviews of Geophysics*, *37*(1), 1–64.

Marshall, J., J. R. Scott, A. Romanou, M. Kelley, & A. Leboissetier (2017), The dependence of the ocean's MOC on mesoscale eddy diffusivities: a model study, *Ocean Modelling*, *111*, 1–8.

Marshall, J., & K. Speer (2012), Closure of the meridional overturning circulation through southern ocean upwelling, *Nature Geoscience*, *5*(3), 171.

Martin,, P., R. S. Lampitt, M. J. Perry, R. Sanders, C. Lee, & E. D'Asaro (2011), Export and mesopelagic particle flux during a North Atlantic spring diatom bloom, *Deep Sea Research Part I: Oceanographic Research Papers*, *58*(4), 338–349.

Martin, A. P., M. I. Lucas, S. C. Painter, R. Pidcock, H. Prandke, H. Prandke, & M. C.Â. Stinchcombe (2010), The supply of nutrients due to vertical turbulent mixing: A study at the porcupine abyssal plain study site in the northeast Atlantic, *Deep Sea Research Part II: Topical Studies in Oceanography*, *57*(15), 1293–1302.

Mashayek, A., R. Ferrari, S. Merrifiield, J. R. Ledwell, L. St Laurent, & A. N. Garabato (2017), Topographic enhancement of vertical turbulent mixing in the southern ocean, *Nature Communications*, *8*, 14, 197.

McClain, C. R., L. J. Pietrafesa, & J. A. Yoder (1984), Observations of Gulf Stream-induced and wind-driven upwelling in the Georgia bight using ocean color and infrared imagery, *Journal of Geophysical Research: Oceans*, *89*(C3), 3705–3723.

McClean, J. L., et al. (2011), A prototype two-decade fully-coupled fine-resolution ccsm simulation, *Ocean Modelling*, *39*(1-2), 10–30.

McGillicuddy, D., L. Anderson, S. Doney, & M. Maltrud (2003), Eddy-driven sources and sinks of nutrients in the upper ocean: Results from a 0.1 resolution model of the North Atlantic, *Global Biogeochemical Cycles*, *17*(2).

McKinley, G. A., D. J. Pilcher, A. R. Fay, K. Lindsay, M. C. Long, & N. S. Lovenduski (2016), Timescales for detection of trends in the ocean carbon sink, *Nature*, *530*(7591), 469.

Melet, A., S. Legg, and R. Hallberg (2016), Climatic impacts of parameterized local and remote tidal mixing, *Journal of Climate*, *29*(10), 3473–3500.

Mertens, C., M. Rhein, M. Walter, C. W. Böning, E. Behrens, D. Kieke, et al. (2014), Circulation and transports in the Newfoundland Basin, western subpolar North Atlantic, *Journal of Geophysical Research: Oceans*, *119*(11), 7772–7793, doi: 10.1002/2014JC010019.

Moore, J. K., K. Lindsay, S. C. Doney, M. C. Long, & K. Misumi (2013), Marine ecosystem dynamics and biogeochemical cycling in the community Earth system model [CESM1 (BGC)]: Comparison of the 1990s with the 2090s under the RCP4.5 and RCP8.5 scenarios, *Journal of Climate*, *26*(23), 9291–9312.

Nagai, T., D. Hasegawa, T. Tanaka, H. Nakamura, E. Tsutsumi, R. Inoue, & T. Yamashiro (2017), First evidence of coherent bands of strong turbulent layers associated with high-wavenumber internal-wave shear in the upstream Kuroshio, *Scientific Reports*, *7*(1), 14,555.

Nagai, T., A. Tanndon, H. Yamazaki, & M. J. Doubell (2009), Evidence of enhanced turbulent dissipation in the frontogenetic Kuroshio Front thermocline, *Geophysical Research Letters*, *36*(L12609).

Nagai, T., A. Tandon, H. Yamazaki, M. J. Doubell, & S. Gallager (2012), Direct observations of microscale turbulence and thermohaline structure in the Kuroshio Front, *Journal of Geophysical Research*, *117*, C08,013.

Oakey, N., & J. Elliott (1977), Vertical temperature gradient structure across the Gulf Stream, *Journal of Geophysical Research*, *82*(9), 1369–1380.

Olson, D. B. (2001), Biophysical dynamics of western transition zones: a preliminary synthesis, *Fisheries Oceanography*, *10*(2), 133–150.

Omand, M. M., & A. Mahadevan (2013), Large-scale alignment of oceanic nitrate and density, *Journal of Geophysical Research: Oceans*, *118*(10), 5322–5332.

Oschlies, A. (2002a), Can eddies make ocean deserts bloom? *Global Biogeochemical Cycles*, *16*(4), 53–1.

Oschlies, A. (2002b), Nutrient supply to the surface waters of the North Atlantic: A model study, *Journal of Geophysical Research: Oceans* (1978–2012), *107*(C5), 14-1–14-13.

Palter, J., & S. Lozier (2008), On the source of Gulf Stream nutrients., *Journal of Geophysical Research*, *113*, C06,018, doi: 10.1029/2007JC004611.

Palter, J. B., I. Marinov, J. L. Sarmiento, & N. Gruber (2013), Large-scale, persistent nutrient fronts of the world ocean: Impacts on biogeochemistry. In I.M. Belkin (ed.), *The handbook of environmental chemistry*, Springer, Berlin, Heidelberg, doi: 10.1007/698_2013_241.

Palevsky, H., & D. P. Nicholson (2018), The North Atlantic biological pump: Insights from the Ocean Observatories Initiative Irminger Sea Array, *Oceanography*, *31*(1), 42–49.

Pelegrí, J. L., & G. T. Csanady (1991), Nutrient transport and diapycnal mixing in the Gulf Stream., *Journal of Geophysical Research*, *96*, 2577–2583, doi: 10.1029/90JC02535.

Pelegrí, J. L., & G. T. Csanady (1994), Diapycnal mixing in western boundary currents., *Journal of Geophysical Research*, *99*, 18,275–18,304, doi: 10.1029/94JCC01201.

Pelegrí, J. L., G. T. Csanady, & A. Martins (1996), The North Atlantic nutrient stream, *Journal of Oceanography*, *52*, 275–299.

Pelegrí, J. L., A. Marrero-Díaz, & A. W. Ratsimandresey (2006), Nutrient irrigation of the North Atlantic, *Progress in Oceanography*, *70*, 366–406.

Polzin, K., & Y. Lvov (2011), Toward regional characterizations of the internal wave field, *Reviews of Geophysics*, *49*(4), doi: 10.1029/2010RG000329.

Reid, J. L. (1994), On the total geostrophic circulation of the North Atlantic ocean: Flow patterns, tracers, and transports, *Progress in Oceanography*, *33*(1), 1–92.

Renault, L., M. J. Molemakerr, J. Gula, S. Masson, & J. C. McWilliams (2016), Control and stabilization of the Gulf Stream by oceanic current interaction with the atmosphere, *Journal of Physical Oceanography*, *46*(11), 3439–3453.

Riahi, K., S. Rao, V. Krey, C. Cho, V. Chirkov, G. Fischer, et al. (2011), Rcp 8.5—a scenario of comparatively high greenhouse gas emissions, *Climatic Change*, *109*(1–2), 33.

Rintoul, S. R., & C. Wunsch (1991), Mass, heat, oxygen and nutrient fluxes and budgets in the North Atlantic ocean, *Deep Sea Research Part A. Oceanographic Research Papers*, *38*, S355–S377.

Rosssby, C. G. (1936), Dynamics of steady ocean currents in light of experimental fluid mechanics, *Papers in Physical Oceanography and Meteorology*, *5*, 1–43.

Rossby, T. (1996), The North Atlantic current and surrounding waters: At the crossroads, *Reviews of Geophysics*, *34*(4), 463–481.

Saba, V. S., S. M. Griffies, W. G. Anderson, M. Winton, M. A. Alexander, T. L. Delworth, et al. (2016), Enhanced warming of the northwest Atlantic ocean under climate change, *Journal of Geophysical Research: Oceans*, *121*(1), 118–132.

Sanders, R., et al. (2014), The biological carbon pump in the North Atlantic, *Progress in Oceanography*, *129*, 200–218.

Sarmiento, J., N. Gruber, M. Brzezinski, & J. Dunne (2004), High-latitude controls of thermocline nutrients and low latitude biological productivity, *Nature*, *427*(6969), 56–60.

Schmittner, A. (2005), Decline of the marine ecosystem caused by a reduction in the Atlantic overturning circulation, *Nature*, *434*(7033), 628.

Schmitz, W. J., & M. S. McCartney (1993), On the North Atlantic circulation, *Reviews of Geophysics*, *31*(1), 29–49.

Schmitz, W. J., & P. L. Richardson (1991), On the sources of the Florida current, *Deep Sea Research Part A. Oceanographic Research Papers*, *38*, S379–S409.

Schoonover, J., W. Dewar, N. Wienders, J. Gula, J. C. McWilliams, M. J.Molemaker, et al. (2016), North Atlantic barotropic vorticity balances in numerical models, *Journal of Physical Oceanography*, *46*(1), 289–303.

Siegel, D. A., K. O. Buesseler, S. C. Doney, S. F. Sailley, M. J. Behrenfeld, & P. W. Boyd (2014), Global assessment of ocean carbon export by combining satellite observations and food-web models, *Global Biogeochemical Cycles*, *28*(3), 181–196.

Small, R., S. Xie, L. O'Neill,, H. Seo, Q. Song, P. Cornillon, et al. (2008), Air–sea interaction over ocean fronts and eddies, *Dynamics of Atmospheres and Oceans*, *45*(3–4), 274–319.

Smith, R., P. Jones, B. Briegleb, F. Bryan, G. Danabasoglu, J. Dennis, J. Dukowicz, et al. (2010), The Parallel Ocean Program (POP) reference manual ocean component of the community climate system model (CCSM) and community Earth system model (CESM), Technical Report LAUR-10–01853, National Center for Atmospheric Research, Boulder, CO, http://www.cesm.ucar.edu/models/cesm1.0/pop2/doc/sci/POPRefManual.pdf (last accessed 13 February 2019).

Sommer, U., & A. Lewandowska (2011), Climate change and the phytoplankton spring bloom: warming and overwintering zooplankton have similar effects on phytoplankton, *Global Change Biology*, *17*(1), 154–162.

Steinacher, M., F. Joos1, T. L. Frölicher, L. Bopp, P. Cadule, V. Cocco, et al. (2010), Projected 21st century decrease in marine productivity: a multi-model analysis, *Biogeosciences*, *7*(3), 979–1005.

Stock, C. A., J. G. John, R. R. Rykaczewski, R. G. Asch, W. W. L. Cheung, J. P. Dunne, et al. (2017), Reconciling fisheries catch and ocean productivity, *Proceedings of the National Academy of Sciences of the USA*, *114*(8), E1441–E1449.

Stommel, H. M. (1958), *The Gulf Stream: a physical and dynamical description*, University of California Press.

Thomas, L. N., J. Taylor, R. Ferrari, & T. Joyce (2013), Symmetric instability in the Gulf Stream., *Deep Sea Research II*, *91*, 96–110.

Thomas, L. N., J. R. Taylor, E. A. D'Asaro, C. M. Lee, J. M. Klymak, & A. Shcherbina (2016), Symmetric instability, inertial oscillations, and turbulence at the Gulf Stream front, *Journal of Physical Oceanography*, *46*(1), 197–217.

Toggweiler, J., & B. Samuels (1998), On the oceans large-scale circulation near the limit of no vertical mixing, *Journal of Physical Oceanography*, *28*(9), 1832–1852.

Van Vuuren, D. P., et al. (2011), The representative concentration pathways: an overview, *Climatic Change*, *109*(1–2), 5.

Waterhouse, A. F., J. A. MacKinnon, J. D. Nash, M. H. Alford, E. Kunze, H. L. Simmons, et al. (2014), Global patterns of diapycnal mixing from measurements of the turbulent dissipation rate, *Journal of Physical Oceanography*, *44*(7), 1854–1872.

Waterman, S., & B. J. Hoskins (2013), Eddy shape, orientation, propagation, and mean flow feedback in western boundary current jets, *Journal of Physical Oceanography*, *43*(8), 1666–1690.

Waterman, S., & S. R. Jayne (2012), Eddy-driven recirculations from a localized transient forcing, *Journal of Physical Oceanography*, *42*(3), 430–447.

Watson, A. J., J. R. Ledwell, M.-J. Messias, B. A. King, N. Mackay, M. P. Meredith, et al. (2013), Rapid cross-density ocean mixing at mid-depths in the drake passage measured by tracer release, *Nature*, *501*(7467), 408.

Weaver, A. J., J. Sedláček, M. Eby, K. Alexander, E. Crespin, T. Fichefet, et al. (2012), Stability of the Atlantic meridional overturning circulation: A model intercomparison, *Geophysical Research Letters*, *39*(20).

Wessel, P., & W. H. Smith (1996), A global, self-consistent, hierarchical, high-resolution shoreline database, *Journal of Geophysical Research: Solid Earth*, *101*(B4), 8741–8743.

Whalen, C. B., J. A. MacKinnon, L. D. Talley, & A. F. Waterhouse (2015), Estimating the mean diapycnal mixing using a fine scale strain parameterization, *Journal of Physical Oceanography*, *45*(4), 1174–1188.

Whalen,, C. B., L. D. Talley, & J. A. Mackinnon (2012), Spatial and temporal variability of global ocean mixing inferred from argo profiles., *Geophysical Research Letters*, *39*(L18612).

While, J., & K. Haines (2010), A comparison of the variability of biological nutrients against depth and potential density, *Biogeosciences*, *7*(4), 1263–1269.

Whitt, D. (2015), Near-inertial waves in oceanic fronts: from generation to dissipation, Ph.D. thesis, Stanford University.

Whitt, D., & L. Thomas (2013), Near-inertial waves in strongly baroclinic currents, *Journal of Physical Oceanography*, *43*, 706–725.

Whitt, D., J. Taylor, & M. Lévy (2017), Synoptic-to-planetary scale wind variability enhances phytoplankton biomass at ocean fronts, *Journal of Geophysical Research: Oceans*, *122*(6), 4602–4633.

Whitt, D. B., L. N. Thomas, J. M. Klymak, C. M. Lee, & E. A. D'Asaro (2018), Interaction of superinertial waves with submesoscale cyclonic filaments in the north wall of the Gulf Stream, *Journal of Physical Oceanography*, *48*(1), 81–99.

Williams, R. G., & M. J. Follows (2003), Physical transport of nutrients and the maintenance of biological production. In M. Fascham (Ed.), *Ocean Biogeochemistry* (19–51), Springer.

Williams, R. G., E. McDonagh, V. M. Roussenov, S. Torres-Valdes, B. King, R. Sanders, & D. A. Hansell (2011), Nutrient streams in the North Atlantic: Advective pathways of inorganic and dissolved organic nutrients, *Global Biogeochemical Cycles*, *25*(4).

Williams, R. G., A. J. McLaren, & M. J. Follows (2000), Estimating the convective supply of nitrate and implied variability in export production over the North Atlantic, *Global Biogeochemical Cycles*, *14*(4), 1299–1313.

Williams, R. G., V. Roussenov, & M. J. Follows (2006), Nutrient streams and their induction into the mixed layer, *Global Biogeochemical Cycles*, *20*(1), GB1016.

Winkel, D. P., M. C. Gregg, & T. B. Sanford (2002), Patterns of shear and turbulence across the Florida current., *Journal of Physical Oceanography*, *32*, 3269–3285.

Winton, M., W. G. Anderson, T. L. Delworth, S. M. Griffies, W. J. Hurlin, & A. Rosati (2014), Has coarse ocean resolution biased simulations of transient climate sensitivity? *Geophysical Research Letters*, *41*(23), 8522–85229.

Yeager, S. (2015), Topographic coupling of the Atlantic overturning and gyre circulations, *Journal of Physical Oceanography*, *45*(5), 1258–1284.

Zhang, J.-Z., M. O. Baringer, C. J. Fischer, et al. (2017), An estimate of diapycnal nutrient fluxes to the euphotic zone in the Florida Straits, *Scientific Reports*, *7*(1), 16,098.